

~~Global basic landform units~~ A typology of global relief classes derived from ~~multi-source~~ digital elevation models at 1 arc-second resolution

Xin Yang^{1,2,3,5†}, Sijin Li^{1,2,3,5†}, Junfei Ma^{1,2,3,5}, Yang Chen^{1,2,3,5}, Xingyu Zhou^{1,2,3,5}, Fayuan Li^{1,2,3,5}, Liyang Xiong^{1,2,3,5},
Chenghu Zhou⁴, Guoan Tang^{1,2,3,5*} & Michael E. Meadows^{6,7*}

[†] These authors contributed equally to this work.

^{*} Co-corresponding authors: Guoan Tang tanggaoan@njnu.edu.cn; Michael E Meadows michael.meadows@uct.ac.za

¹State Key Laboratory of Climate System Prediction and Risk Management, Nanjing Normal University, Nanjing 210023, China

²School of Geography, Nanjing Normal University, Nanjing, 210023, China

³Key Laboratory of Virtual Geographic Environment (Nanjing Normal University), Ministry of Education, Nanjing, 210023, China

⁴Institute of Geographical Information Science and Natural Resources, Chinese Academy of Science, Beijing, 100101, China

⁵Jiangsu Centre for Collaborative Innovation in Geographical Information Resource Development and Application, Nanjing 210023, China

⁶School of Geography and Ocean Sciences, Nanjing University, Nanjing 210023, China

⁷Department of Environmental & Geographical Science, University of Cape Town, Rondebosch 7701, South Africa

Abstract. Understanding the land surface morphology and its relief components, which record the dynamics of the planet's evolution and interaction of multiple environmental factors, constitutes a critical aspect of Earth system science. Landforms are fundamental components of the Earth surface, providing the base on which surface processes operate. Understanding and classifying global landforms, which record the internal and external dynamics of the planet's evolution, constitutes a critical aspect of Earth system science. Advances in Earth observation technologies have enabled access to higher resolution data, for example, remote sensing imagery and digital elevation models (DEMs). However, classified landform-relief and landform data with a resolution of approximately 1 arc-second (approximately 30 m) are lacking at the global scale, which limits the progress of geomorphologic related studies at finer scales. Here, we propose a novel framework for global landform-relief classification and release a unique dataset called Global-global Basic-relief Landform-Unitsclasses (GBLUGRC), which incorporates a comprehensive set of objects that constitute the range of landforms-terrains and landforms on Earth. Constructed from multiple 1 arc-second DEMs, GBLUGRC covers global land and ranks among the highest-resolution global geomorphic geomorphology-datasets to date. Its development integrates geomorphological-land surface ontologies, with core, transitions and boundaries, and key derivatives to strike a balance between mitigating local noise and preserving valuable landform details. GBLUGRC categorizes the Earth's landforms-land relief into three levels with 26 classes two levels, yielding raster files and discrete vector units that record landform-relief type and distribution. Comparative analyses with previous datasets reveal that GBLUGRC enhances-is beneficial in capturing of landform details of surface morphology, enabling more precise depiction of geomorphological boundaries. This refinement facilitates the identification of finer and novel more precise spatial disparities in landform patterns than before, exemplified by marked contrasts between Asia and other continents, and highlights the distinct prominence of Peru and China in terms of landform-relief diversity. Given that the fundamental-data resolution of GBLUGRC accords well with available-accessible remote sensing imagery and other Earth scientific datasets, it is readily incorporated into analytical workflows, exploring the relationship between landformsland morphology, surface runoff, climate and land cover. The full data set is available on the Deep-time Digital Earth Geomorphology platform and Zenodo (Yang et al., 2024; <https://doi.org/10.5281/zenodo.15641257><https://doi.org/10.5281/zenodo.13187969>).

1. Introduction

Approaches to geomorphology vary, and include research on, for example, genesis, processes, materials, hazard and risk, and chronology, but the essential basis of all of these studies is the landform (Evans, 2012), which can be regarded as the 'final surface status' resulting from the combined influence of various forces. The morphology of landforms and their associated evolutionary processes have long been a source of fascination, leading ultimately to the development of the formal science of geomorphology (MacMillan and Shary, 2009). Classifying and mapping the Earth's surface into landform types according to morphological characteristics is a primary means of understanding surface patterns and processes on planet Earth (Evans, 2012; Xiong et al., 2022) and advancement in this field has potential benefits for the more efficient allocation of global resources to promote sustainable development (Dramis, 2009). Understanding the morphology of the Earth's surface and its constituent types is one of the fundamental

tasks of Earth system science (Evans, 2012; Pepin et al., 2022). In this domain, surface relief is a significant characteristic, ~~which~~ playing a critical role in regulating energy flows and material transport across terrestrial environments and exerting significant influence on geomorphic evolution, hydrological balance, and human activity (Thornton et al., 2022; Viviroli et al., 2020; Xiong et al., 2023; Zhou and Chen, 2025). Although different disciplines may adopt varying terminologies—such as “landform,” “terrain,” or “relief class” (Drăguț and Eisank, 2012; Meybeck et al., 2001; Thornton et al., 2021; Viviroli et al., 2020)—to describe these morphological features, their conceptual essence remains broadly consistent: to represent spatial patterns of vertical variation that shape the Earth’s surface and influence key environmental processes. Classifying and mapping the Earth’s surface into relief classes according to morphological characteristics is a primary means of understanding surface patterns and processes on planet Earth (Evans, 2012; Xiong et al., 2022) and advancement in this field has potential benefits for the more efficient allocation of global resources to promote sustainable development (Dramis, 2009).

Traditional ~~landform~~ mapping of relief classes primarily relies upon manual interpretation, ~~the~~ survey based on the field work, topographic maps and aerial photographs supported by field investigations (Drăguț and Blaschke, 2006; Hammond, 1954; Iwahashi et al., 2018; Pennock et al., 1987). ~~However,~~ a series of technological developments has facilitated the automation of ~~landform~~ classification in recent decades, largely dependent on topographic derivatives calculated from DEMs, such as slope, aspect, relief, curvature, ~~and~~ roughness (Jasiewicz and Stepinski, 2013; Amatulli et al., 2018, 2020; Dyba and Jasiewicz, 2022; Snethlage et al., 2022). With the development of earth observation systems and DEM refinement, several global ~~landform~~ datasets based on this framework have been proposed using various data sources and at different levels of spatial resolution (Florinsky, 2017; Iwahashi and Yamazaki, 2022). Using a decision tree algorithm and 1-km SRTM30 data, Iwahashi and Pike (2007) generated a global terrain classification gridded dataset containing 16 undefined topographic types determined by slope gradient, local convexity, and surface texture. Relying on elevation and the standard deviation of elevation, Drăguț and Eisank (2012) adopted an object-based method to automatically classify global landforms from SRTM data resampled to 1 km. Meanwhile, Iwahashi et al. (2018) improved their previous work and established 15 ~~landform~~ classes based on MERIT DEM. ~~To further eliminate issues involved in detecting narrow valley bottom plains, metropolitan areas, and slight inclines in otherwise largely flat plains, Iwahashi and Yamazaki (2022) introduced the elevation above the nearest drainage line measure, and achieved~~ ~~landform~~ land surface classification based on a DEM at 90m resolution. ~~However, as the authors stated, unsupervised classification-based methods to perform higher resolution global landform classification require an international team with knowledge of geomorphological development in a variety of climatic and physiographic settings (Iwahashi and Yamazaki, 2022).~~ In addition, at regional and ~~for~~ global scales, several researchers have achieved automated ~~landform~~ classification methods following the Hammond procedure (Gallant et al., 2005; Karagulle et al., 2017; Martins et al., 2016). All these datasets have provided valuable resources to explore surface patterns, and also played important roles in supporting related disciplines such as hydrology, pedology, and ecology ~~among others~~.

However, shortfalls remain in current relief and landform classification research and require attention to the following points.

Firstly, most previous studies have adopted relatively coarse resolution DEMs, resulting in an inaccurate depiction of topographic morphological information. Recent developments in Earth observation technology have concentrated on the deployment of digital elevation models (DEMs), which contain abundant geometric information about surface relief (Drăguț and Eisank, 2011), although the approach and methods of implementing relief landform-classification have not kept pace with advances in DEM resolution and quality. ~~Nevertheless,~~ Hhigher DEM data resolution can be regarded as a double-edged sword, in that it at once provides the opportunity for landform-relief class mapping at a finer scale while at the same time increasing the challenge of reducing the negative effect of the data noise and abrupt terrain variations (Jasiewicz and Stepinski, 2013) and maintaining the morphological integrity of the identified landformsobjects. Secondly, at the global scale, diverse and complex environmental factors ~~have~~ increase the complexity of landform-land surface morphology -that poses substantial challenges to the generalizability of classification methods (Li et al., 2020). With increasing human impact on landformsland surface, a re-evaluation of relief and landform classification that takes advantage of an increasingly potent digital database and ongoing improvements in human understanding of landform evolutionland surface morphology and processes seemsseems opportune. Finally, landform-geomorphic ainformation obtained from a particular metric is derived at a particular spatial scale, determined jointly by the DEM resolution and window size in the neighborhood analysis, giving rise to uncertainties in the landform-classification results.

Therefore, the development of innovative classification approaches and systems based on high-high-resolution DEMs remains a priority for research on global relief classes and landforms. In this study, we conduct a classification and mapping of global landforms-relief classes based on a DEM at 1 arc-second resolution. We focus on the classification of ~~basic landforms geomorphologiegeomorphic objects~~ that emphasizes morphological differences and, in so doing, we present the practical expression of landform-object ontology at the global scale that offers valuable insights into the Earth's surface structure comprising the constellation of landform-relief types and their boundaries. The objectives of this research are: (1) to construct a global classification system and framework for landforms-land relief classes that integrates domain consideration of landform-related studies, ~~(2) to design a novel framework for global basic landform classification,~~ ~~(3) to develop an automated classification and mapping model~~ for global landformsrelief classes, and ~~(4) to make available a comprehensive global dataset of~~ landform-relief units.

2. Methodology

2.1 Hierarchical classification system and data

In aiming to provide a comprehensive classification of relief and landforms-landform classes at the global scale, our study encompasses all terrestrial regions worldwide, including islands and polar areas. Identifying landform-objects and constructing a classification system is a preliminary and significant step in ~~geomorphological and landform-classification related~~ studies. It is crucial to recognize that land surface objects ~~landforms~~ not only represent assemblages of quantitative characteristics but also convey the basic human understanding of nature (Smith and Mark, 2001). For example, the identification of what is acknowledged as a 'mountain' is as much a product of human perception as of its natural characteristics (Smith and Mark, 2003), thus emphasizing

the importance of incorporating human understanding and domain application into relief landform-classification and mapping. In this study, we focus here on the classification of basic landform relief classes that emphasizes vertical variation and relief intensity across different landforms ~~morphological differences~~ that are not only perceptible to humans but also constitute vital components in the analysis of surface environments.

In taking into consideration the complexity of global landform-topographic characteristics, the classification criteria should satisfy the following requirements: (1) the determined classes should be globally applicable; (2) the -setting of relief classes of the landform types should conform with the current knowledge domain of geomorphology-the Earth system science; and (3) specific criteria should be able to be interpreted and applied. ~~The term "landform" is inherently scale and context dependent. In this study, we specifically emphasize force accumulation, mountain ecosystems, and microclimatic gradients before constructing the classification system.~~ After a comprehensive consideration of numerous previous classification systems (Meybeck et al., 2001; Zhou et al., 2009), we propose a set of criteria for basic landform relief classification, ~~primarily based on~~ (Zhou et al., 2009). The new criteria integrate the typical rules of relief and landform classification with indices proposed in this work, and are aimed at reflecting human knowledge in a quantitative way. We establish a hierarchical classification system comprising 3-2 levels and 23-9 classes (Table A1), thereby advancing a structured framework for understanding Earth's diverse landscapes. The first-level (L1) corresponds to the conventional concept of a complete landform entity, while the second level (L2) provides progressively finer-scale morphological information. The L1 classification primarily aims to distinguish broadly distributed rugged uplands and their counterpart—flat lowlands (Meybeck et al., 2001; Viviroli et al., 2020). To ensure clarity and interdisciplinary compatibility, we deliberately avoided using terms in a strict geomorphological sense (e.g., "mountain," "plain") and instead adopted extended geographic terms. In this study, we refer to the two primary surface types as flat land flat terrain and rugged land rugged terrain, based on their differences in slope characteristics. While flat land flat terrain and rugged land rugged terrain largely correspond to traditional concepts of plains and mountains, respectively, they are defined based on quantifiable morphological characteristics, thereby offering a more flexible and reproducible framework. These two contrasting relief classes provide essential support for understanding landform processes, analyzing hydrological patterns, and assessing the spatial distribution of human activities across diverse environmental contexts (Viviroli et al., 2020). This classification perspective aids researchers in conducting macro-scale studies. At L2, the flat land flat terrain retained elevation-based characteristics and areis further divided into low-altitude, middle-altitude, high-altitude, and very high-altitude flat land flat terrain. The rugged lands are Rugged terrain is subdivided at L2 into low-relief, gentle-relief, moderate-relief, high-relief and very high-relief rugged land rugged terrain.

~~The first level (L1) corresponds to the conventional concept of a complete landform entity, while the second level (L2) and third level (L3) provide progressively finer scale morphological information. L1 types are defined as 'plain' and 'mountain', reflecting the most fundamental morphological characteristics of landforms. Plains and mountains are the most direct reflection of the combined effects of geomorphological processes and profoundly influence biological activities. This classification perspective~~

~~aids researchers in conducting macro-scale studies. At L2, plain landforms retain their labels to guarantee completeness of the classification system, and are further divided into low altitude, middle altitude, high altitude, and highest altitude plains based on elevation. Mountains are subdivided at L2 into hills and other mountains with varying degrees of relief. At L3, we provide a further detailed classification of hills and mountains based on elevation.~~

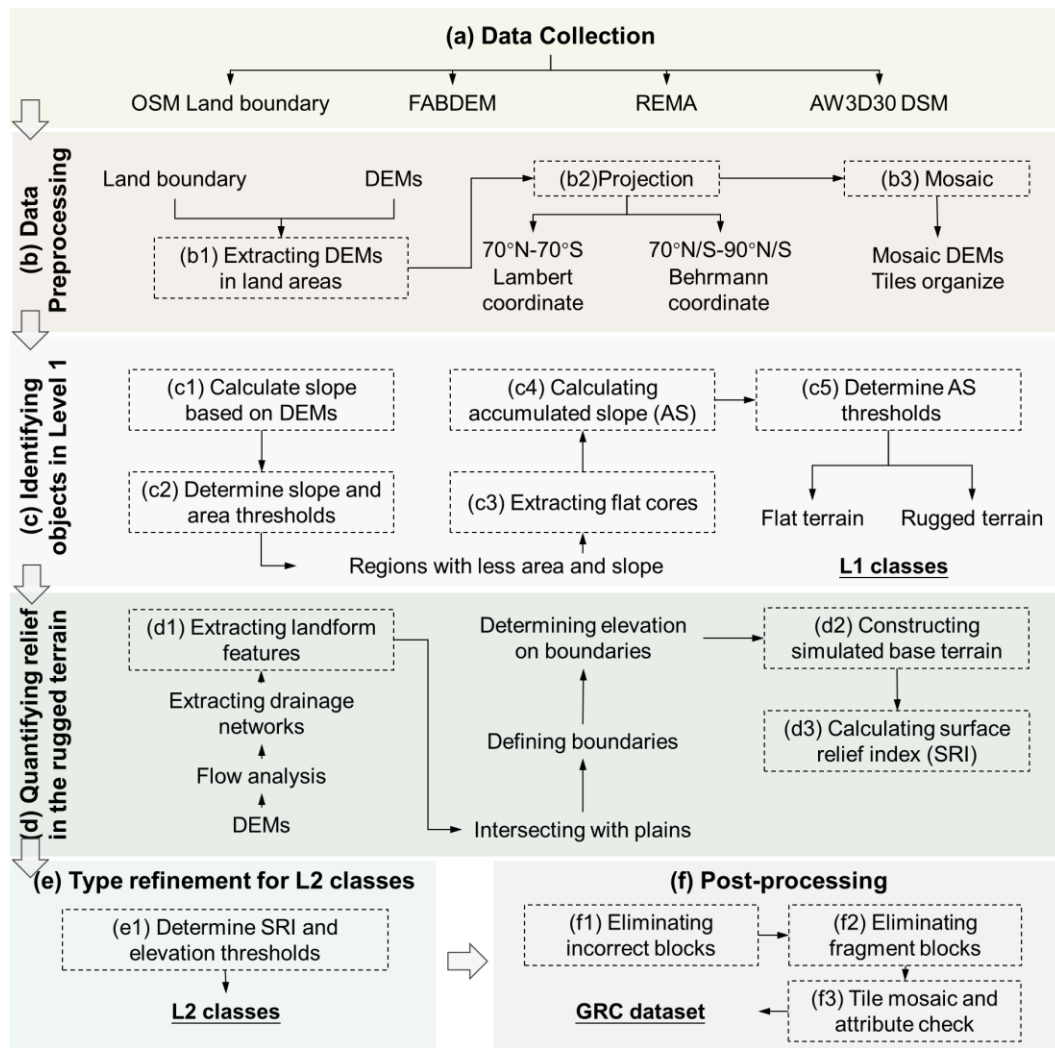
To attain global coverage, we utilize three DEM datasets (Table 1). These datasets are publicly available for access and have been widely used in geomorphological studies, ensuring their accuracy and validity. In this work, the ‘Forest and Buildings removed Copernicus DEM’ (FABDEM) (Hawker et al., 2022) is the primary data for latitudes 60°S-80°N. This dataset is the first bare-earth DEM dataset at a global scale at 1 arc-second (approximately 30-meter) resolution, developed using machine learning techniques from Copernicus DEM. By eliminating the bias resulting from building and vegetation heights, some terrain features, such as slope, aspect, and watersheds, can be estimated more accurately, which is of significant benefit in landform classification. Meanwhile, the Advanced Land Observing Satellite (ALOS) World 3D - 30 m (AW3D30) (Tadono et al., 2014) ~~dataset and Reference Elevation Model of Antarctica (REMA) (Howat et al., 2022) is are~~ used to supply data for the area missing from FABDEM. In addition, to avoid the negative impact of ocean pixels on ~~landform~~ classification results, the OpenStreetMap (OSM) Land Polygon was utilized as a mask to eliminate the sea.

Table 1. Data sources and attributes

	FABDEM	AW3D30 V3.2	REMA
Spatial Coverage	60°S-80°N	82°S-82°N	56°S-88°S
Spatial Resolution	1 arc-second	1 arc-second	32 m
Vertical Accuracy	<4 m	4.4 m (RMSE)	4 m (RMSE)
Release Date	2021	2021	2022
Data link	https://data.bris.ac.uk/data/datasets/s5hqmjcdj8yo2ibzi9b4ew3sn	https://www.eorc.jaxa.jp/ALOS/jp/dataset/aw3d30/aw3d30_j.htm	https://www.pgc.umn.edu/data/rema/

2.2 ~~Global Landform e~~Classification method

In this study, we propose a new framework and provide the corresponding implementation workflow. The proposed method ~~of global landform classification~~ has a hierarchical structure, involving data pre-processing, identification of mountains and plains, calculation of the surface relief index (SRI), ~~landform-relief~~ classification, and post-processing. Figure 1 illustrates the workflow. The following sections provide details that should allow users to reproduce our results. In this study, we built characteristic quantification and ~~landform~~ classification models based on tools in ArcGIS Pro. A detailed description of the step-by-step procedures follows below.



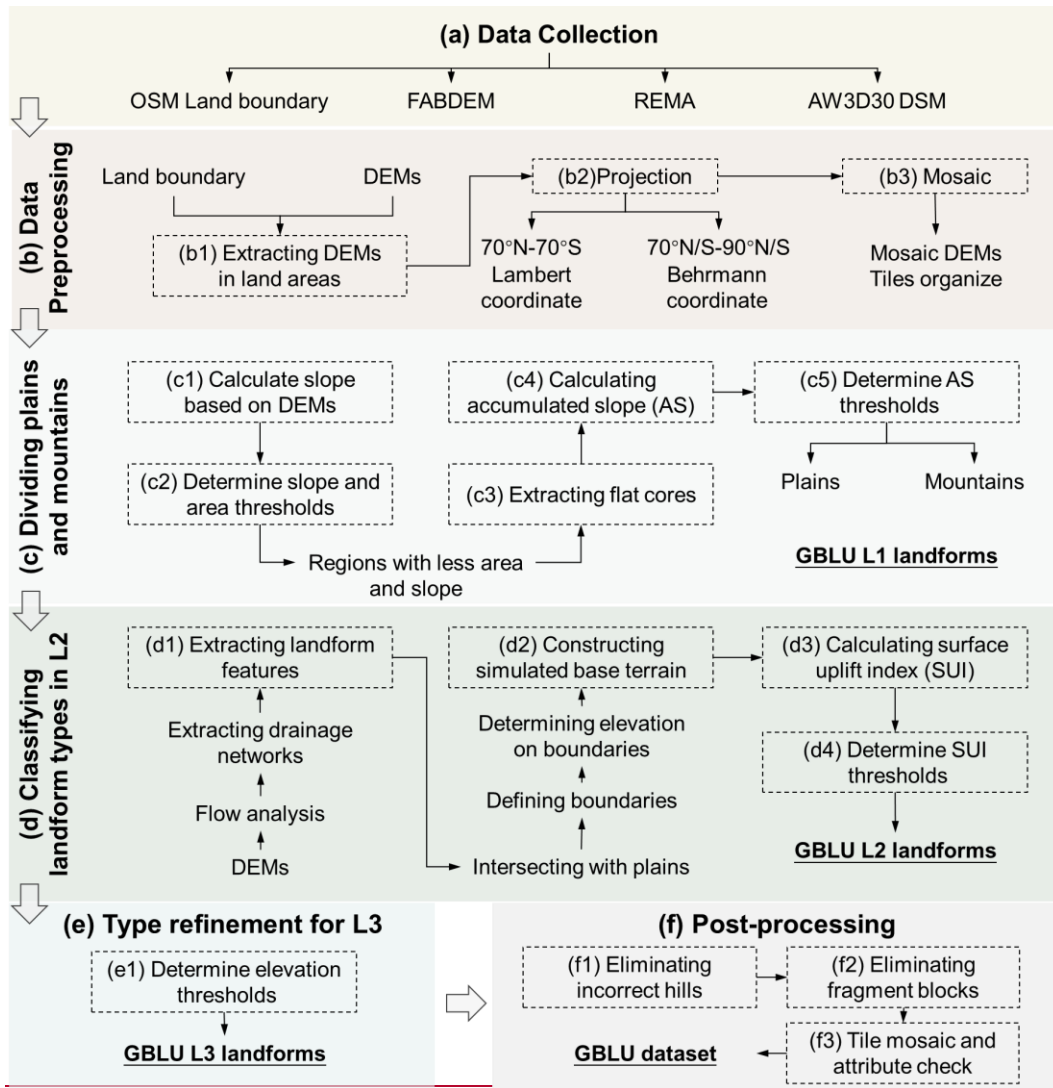


Figure 1. Workflow for global landform classification used in this study of the proposed classification method.

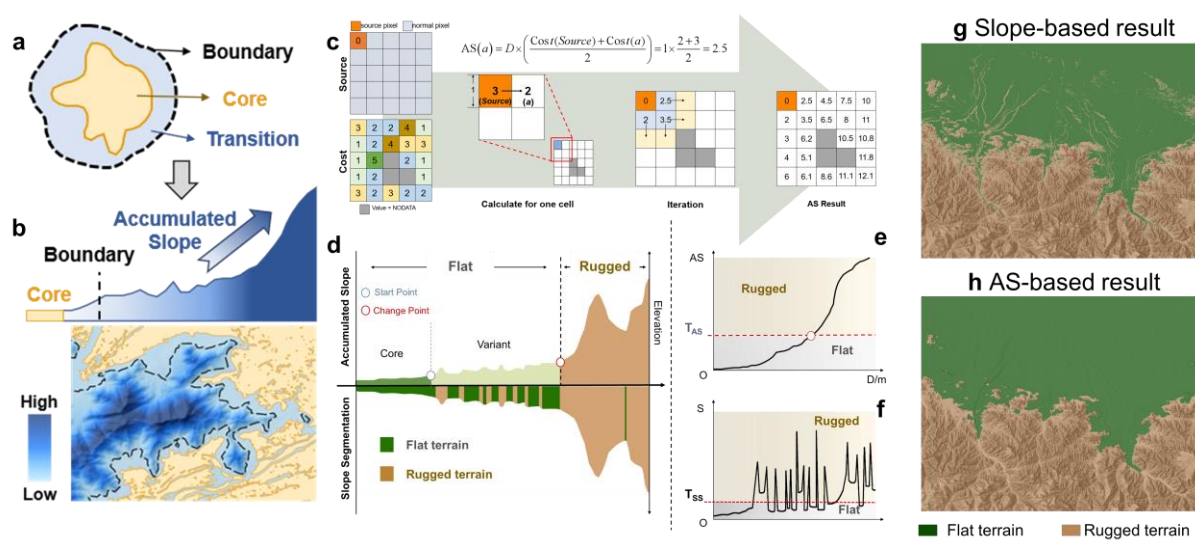
2.2.1 Data preprocessing

As shown in Figure 1b, data pre-processing focuses primarily on land area extraction and data merging. We use the OSM land polygon as the land mask to eliminate the marine pixels that negatively influence subsequent processes. To improve processing efficiency, the original DEM elements with size of 1×1 degree are mosaiced to tiles of 10×10 degrees. Meanwhile, due to the requirement of calculating landform derivatives, we determine the projection principles as follows: Tiles between 70° N/S are reprojected to the equal area Behrmann projection, and the tiles polewards of 70° N/S to Lambert azimuthal equal-area. To mitigate border effects between the two projection zones, we have implemented an overlapping strategy in our processing. Specifically, we processed the DEMs in $11^\circ \times 11^\circ$ tiles, ensuring that the main $10^\circ \times 10^\circ$ area is used as the final output. This approach helps maintain consistency and minimizes distortions at the transition between projection zones. For consistency and ease of use, the final TIFF files have been reprojected into a single coordinate system (EPSG:3857)

2.2.2 Identifying plains and mountains objects in Level 1

Identifying and distinguishing contrasting plains and mountains flat and rugged land rugged terrain represents the initial step in

basic landform classification and mapping in the proposed framework. To achieve this, we propose re-examining classification from an ontological perspective. In information science, an ontology is a neutral and computationally tractable description of a given individual or category which can be accepted and reused by all information gatherers (Smith and Mark, 2003). In this study, based on the spatial information theory, we propose a conceptual description of relief objects that enhances the generalization of land surface and reduces the negative influence of vagueness. Considering that the characteristics of flat land terrain are more distinct and their definition is clearer, we will use flat land terrain as the foundation for expanding the relief ontology. As shown in Figure 2a, the conceptual model of flat land terrain includes three elements, viz., core, transition and boundary. The core represents areas with the most typical flat characteristics, i.e. very low slope. Transitions are occur around cores and contain areas with higher slope than typical flat land terrain, i.e. areas that in part satisfy their classification as flat land terrain but also exhibit sloping characteristics not typical of flat land terrain. In a general geographic context, these areas should also be classified as flat land terrain. However, current methods that emphasize local topographic characteristics often fail to identify them correctly. The boundary is defined as the spatial margin of the flat land terrain where topographic properties and classification labels shift gradually toward those associated with rugged terrain. In this context, misclassification tends to occur in transitional zones, which exhibit mixed topographic features that do not fully align with either flat or rugged land rugged terrain characteristics. We have designed a practical framework based on landform ontology to classify plains and mountains these two objects. The plains can be separated into core, transition and boundary, whereby the core represents areas with the most typical flat characteristics, i.e. very low relief. Transitions have plain cores but also contain sloping elements, i.e. areas that in part satisfy their classification as plain but also exhibit sloping characteristics not typical of plain. as shown in Figure 2. Misclassifications usually occur in transition areas due to their atypical characteristics. Meanwhile, the boundary represents the part of the plain area where the geomorphological semantics and labels change to the mountain.



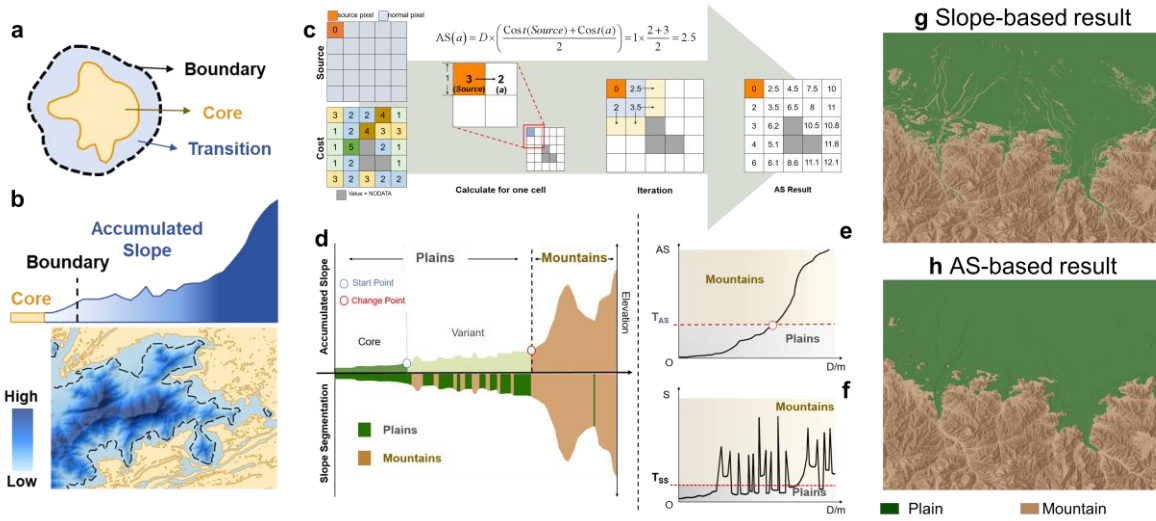


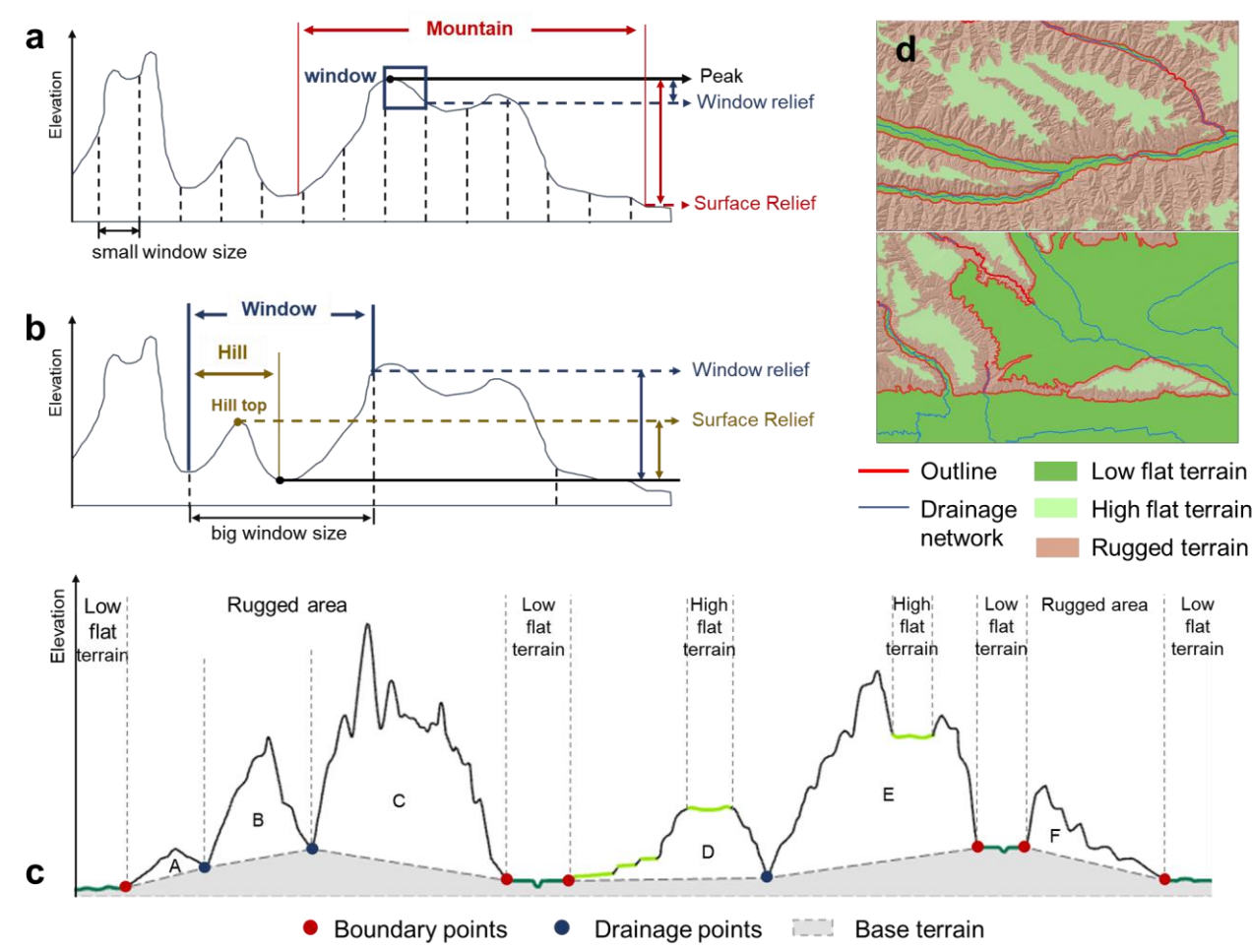
Figure 2. Illustration of calculation methods. **a** Conceptualization of plains flat land flat terrain. **b** calculation principle and results of accumulated slope (AS), respectively. **c** schematic diagram of the cost-distance algorithm. The cost refers to the slope in this process. **d** profile reflecting landform-land surface composition according to the proposed conceptual model-of plains, segmented based on the slope; **e** calculated result of the AS and **f** calculated result of slope, where T_{AS} is the threshold of AS, and T_{SS} is the threshold of surface slope. For Figures 2c and d, areas smaller than the threshold are classified as plains flat land flat terrain (marked in green), while the remaining areas are classified as mountains rugged land rugged terrain (marked in brown). **g** and **h** comparison of the AS and slope indicators in the division of plains and mountains Level 1 classes.

In conducting the classification processes, Firstly, we regard the areas with low slope angles as the plain-flat cores. Here, the slope threshold (T_{SS}) is recommended to be set as 1.5-3-degrees according to our global pre-assessment experiments. Areas where the slope angle lies below the threshold T_{SS} are classified as plain-flat cores. A block must be greater than 0.1 km² to be classified as a core plain area. In landform classification, the core areas of each landform are typically distinct and can be accurately identified. However, there is significant ambiguity in the transitional zones and boundaries between different landform types. To address this issue, we propose reexamining landform classification from an ontological perspective. In information science, an ontology is a neutral and computationally tractable description of a given individual or category which can be accepted and reused by all information gatherers (Smith and Mark, 2003). In this study, based on the spatial information theory, we propose a conceptual description of landforms that enhances the generalization of landform and reduce the negative influence of vagueness. Considering that the characteristics of plains are more distinct and their definition is clearer, we will use plains as the foundation for expanding the landform ontology. As shown in Figure 2a, the conceptual model of plains includes three elements, viz. core, transition and boundary. The plain core represents areas with the most typical plain characteristics, i.e. very low relief. Transitions are areas with elements consistent with the plain cores but also contain non standard slope characteristics. In other words, transitions in part satisfy their identification as plains but also exhibit characteristics that may not be typical of plans, and this may lead to an inaccurate classification. The boundary represents the part of the plain where the geomorphological semantics and labels change. The fundamental characteristics of plains, i.e. flat terrain, are defined as the plain core and quantified by slope angle in the previous step. The other elements are determined based on the cores. For example, as we discussed before noted above, areas outside the plain core that beyond the core have a with relatively low relief should also be considered plains flat land terrain in the geomorphological

geographic sense, although However, segmentation based on slope characteristics may usually fails to identify them as such due to emphasis being placed on local changes in topography (Figure 2g). These introduces patches in the extraction of plains that may fragment the integrity of larger plains. Furthermore Meanwhile, the resulting landscape segments may themselves contain fragments that reflect local topographic changes but do not represent actual landform objects as recognized geomorphologically. It is challenging to correct all such fragments across complex terrain scenarios at the global scale, thus limiting the feasibility of automated global landform-relief classification.

To address these issues, as the second step in our classification process, we introduce the concept of accumulated cost-slope (AS) and develop an AS derivative that quantifies the attributes of plain transitions by calculating the AS along a path that has the lowest slope cost (Figure 2b). In this process, the core is the typical areas extracted in the previous step, and the cost surface is the slope gradient. The AS is calculated as the minimum cumulative cost of each position to the nearest plain-core along a specific path. In the AS calculation of general position, this algorithm employs an iteration starting from the cell closest to the cores and follows the calculation principle shown in Figure 2c to compute the minimum accumulated slope of each cell to the core. The completed area is then expanded until all grids are associated with increasing costs. This process follows the geospatial analysis principle of the minimum accumulated cost (Sechu et al., 2021). The tool of distance accumulation in ArcGIS Pro can achieve this calculation. Segmenting landforms through the determination of the thresholds for landform-topographic derivatives is one of the most common methods used in geomorphological studies and transforms geomorphological-qualitative perception towards quantitative computation. As shown in Figure 2d, due to differences in topographic characteristics between plains-flat and mountains-rugged landterrain, the AS has a low rate of increase in the areas classified as plains-flat landterrains and a high rate of increase in rugged areas. This phenomenon reduces the difficulty of determining an appropriate AS threshold, which can be achieved by searching for abrupt changes in the AS profile. In this step, taking into consideration the geomorphological perspective, the threshold of AS (T_2, T_{AS}) is recommended to be 1500-2000 based on the pre-experimental results conducted on numerous samples worldwide. Areas where the AS value is less than T_{AS} are merged with the cores to form the complete flat landterrain, while the remaining areas are classified as rugged landrugged terrain. This threshold range is provided as a reference but gentle adjustments to the thresholds may be required in some special areas, such as small islands, through human-computer interaction. In some cases, such as small islands where traditional watershed and TIN-based methods tend to struggle, it may exceed the recommended threshold range. Areas where the AS value is less than T_2 are regarded as plains, and the remaining areas are mountains. Through the above segmentation, we can obtain the boundary of plain-flat landsflat terrain and construct the complete flat plain-area consisting of core, variant and boundary. As shown in Figures 2g and h, this novel-workflow exaggerates the difference between the plains-and-mountainsflat and rugged landterrain and converts the local slope into an indicator of global landform-characteristics. This novel method avoids the negative effect of local window analysis and is beneficial for maintaining the landform semantics for each block.

2.2.3 ClassifyingQuantifying landform surface relief types in level 2in the rugged landrugged terrain



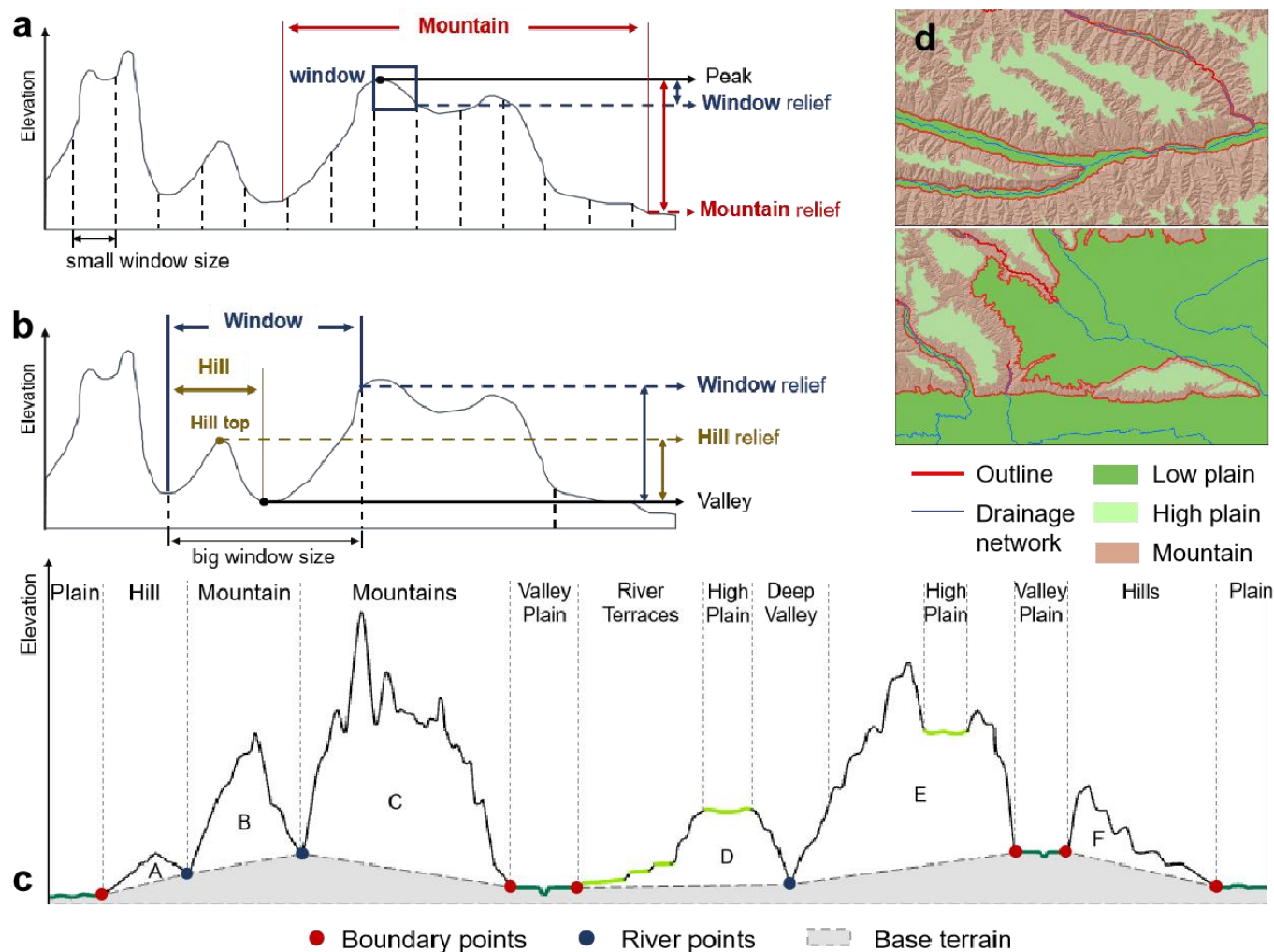


Figure 3. Uncertainty in relief calculation based on the window analysis. a and b the relationship between different windows and topographical-surface relief in rugged areas. c schematic diagram illustrating the base terrain for calculating surface relief index of mountains. d features used to create TIN and build base terrain.

In this step, we focus on the differences of quantifying terrain-relief difference to achieve the comprehensive classification of L2 landform classes. It should be noted that the term terrain relief in this study emphasizes the use of quantitative terrain metrics (i.e., relief index) to measure the degree of vertical variation across the Earth's surface. Terrain relief refers to the difference in elevation between the highest and lowest points within a particular spatial unit. This factor significantly influences landform-land surface classification. However, commonly employed indices reflecting topographic relief are achieved using a window of fixed size such as 3×3 , 5×5 pixels, or larger (Maxwell and Shobe, 2022), a method that fails to account for geomorphological semantics, and which therefore disregards the integrity of a mountain or hill. Window size has a significant impact on the results of relief calculation and quantification. As shown in Figures 3a and b, window analysis tends to disrupt the integrity and continuity of geomorphological elements. Moreover, a small window size is insufficient to capture the entire mountain elements, particularly in the case of large mountains, while a large window size may incorporate other mountains elements and fail effectively to capture the real relief. The uncertainty introduced by window size further increases the difficulty of global classification and mapping based on relief index. Even the multi-scale synthesis approaches can effectively mitigate scale-dependent limitations; these methods still

inherently face challenges associated with determining appropriate scales ranges in algorithms.

Therefore, we propose a new method for relief quantification ~~method~~ which ~~does~~ not rely on the traditional window-based calculation. In this paper, the surface relief index (SRI) is defined as the degree of ~~relative~~ relief relative to the flat areas surrounding ~~the mountain rugged land terrain~~. We regard the elevation at the foot of the ~~mountain rugged land rugged terrain~~ as the base elevation and then calculate the elevation difference between each position on the ~~mountains rugged land rugged terrain~~ and the base elevation. Compared to the traditional method of relief calculation (e.g., difference in elevation within a particular window size), SRI considers the vertical elevation differences between the surface and the ~~mountain~~ base, which is more suitable for ~~the~~ objectives in landform-related studies such as ~~mountainous mountain~~ climate and biodiversity.

This step includes three sub-procedures. Firstly, we constructed the ~~mountain rugged land rugged terrain~~ extent as the foundation for subsequent calculation. The ~~plain flat land flat terrain~~ boundary ~~lies at the foot of landforms classified as mountain, which is suitable to~~ is primarily used to define ~~represent~~ the extent of ~~mountains rugged terrain lands~~. However, when the area of rugged terrain (such as mountains) is large, and the base elevation is constructed solely from the boundary of the flat terrain, the result may not accurately reflect the actual terrain relief. However, when the area of the mountain rugged land (such as mountains) is large, and ~~if~~ the base elevation is constructed only on the basis of the ~~plain flat land~~ boundary, the result cannot reflect the real terrain relief. To refine the representation of surface relief, we introduce linear features representing ~~the~~ rivers. These additional lines can be obtained through ~~DEM-DEM~~-based hydro-analysis (Li et al., 2021). In order to ensure that ~~plains flat lands flat terrain~~ at high elevations ~~does~~ not interfere with the definition of the ~~mountain rugged~~ unit, since ~~these are it is~~, in effect, part of the ~~mountain rugged land rugged terrain~~ range (Figure 3c-). ~~We~~ we exclude high ~~elevation plains altitude flats~~ (marked in light green in Figure 3d) that have no fluvial features to retain the integrity of the associated ~~mountain rugged land rugged terrain~~ range. Figure 3d shows the final elements involved in establishing the base elevation, which corresponds to the boundary of the ~~low low-altitude plains flats~~ and fluvial features (marked in red in Figure 3d). Secondly, we constructed the base elevation to support the calculation of the SRI. In this case, the ~~mountain rugged land rugged terrain~~ extent, which replaces the analysis window in traditional relief calculation, is used to construct the base elevation. ~~Specifically, we construct~~ ~~Specially, we constructed~~ the triangulated irregular network (TIN) based on the position extracted in the first step and then regard the elevation value in TIN as the base elevation. The construction of TIN can be achieved in ArcGIS Pro through ~~create~~ the creation of TIN. Thirdly, the SRI is obtained by calculating the difference between each cell ~~height altitude~~ and its corresponding base elevation. This novel method provides a more appropriate representation of the underlying terrain.

2.2.4 Type refinement for L2 classes

According to the results of previous studies (Meybeck et al., 2001; Zhou et al., 2009), we constructed the classification criteria shown in a Appendix of Table A1. For the flat land terrain, we use altitudes of 1000m, 3500m and 5000m as break points to generate low-, middle-, high- and highest-altitude classes. The rugged lands are Rugged terrain is classified as low-relief, gentle-relief,

moderate-relief, high-relief, and very high-relief classes, based on threshold SRI values of 200m, 1000m, 3500m and 5000m. In all, this yields six classes in L2.

2.2.4 Type refinement for L3

According to the results of previous studies (Zhou et al., 2009), we constructed the classification criteria shown in appendix of Table A1. For the plains, we use altitudes of 1000m, 3500m and 5000m as break points to generate low-, middle-, high- and highest-altitude landforms. Mountains are classified as hill, low-relief, middle-relief, high-relief, and highest-relief mountains, based on threshold SRI values of 200m, 1000m, 3500m and 5000m. In all, this yields 6 classes in L2 and 23 classes in L3.

2.2.5 Post-processing

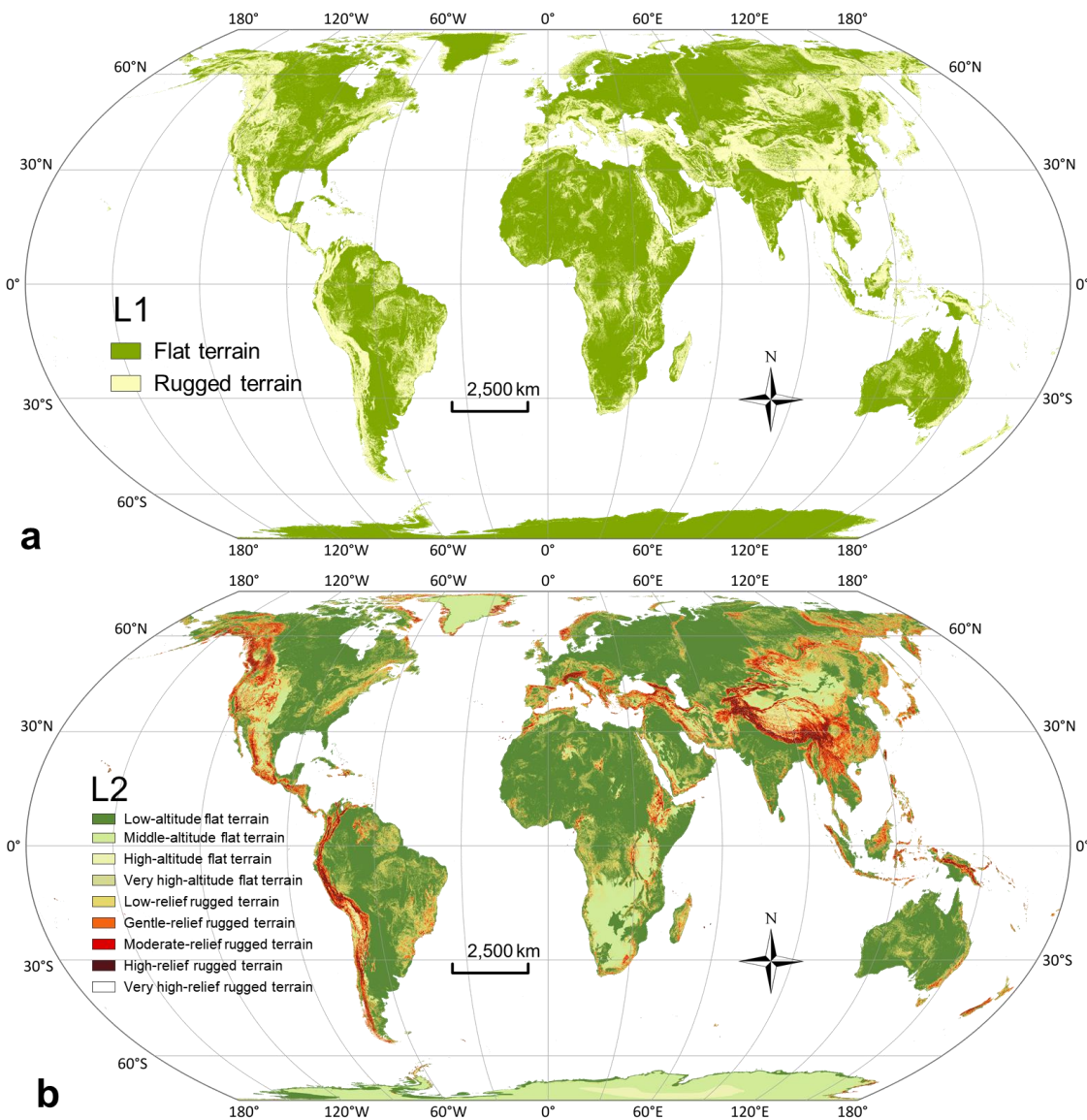
Following the completion of the above processes, a map is generated that includes all the basic landform units/relief classes. However, due to interference caused by the existence of locally steep changes in topographic relief, this output still contains some features in the plain-flat areas misclassified as hills/rugged land/rugged terrain. Meanwhile, although the data we used are/are of high resolution and good quality, outliers and/or data noise remain. Such anomalies may result in small landform blocks with relatively low terrain relief. and, in In accommodating this limitation, we designed an optimization process to correct hill misclassification/these misclassifications. We used area and SRI to reflect/ing their characteristics (e.g., fragmented and relatively low relief). Considering the application of geomorphologic landform data and in geomorphologic mapping and the resolution of basic-fundamental data, we determined that our study corresponds approximately to the equivalent of 1:200,000 geomorphological mapping. Under the conditions of 1:200,000 scale, the minimum displayable patch size is approximately 0.16 km². The SRI threshold is derived from (Zhou et al., 2009), which defines plains as the blocks with relief of less than 30 metres. Therefore, blocks with areas of less than 0.16 km² and SRIs below 30 metres are regarded as misclassified blocks which are then integrated as part of the surrounding plains/flat land/flat terrains.

Meanwhile, we designed an additional step to optimize the results for desert areas. Many arid regions are characterized by dunes, which are distinctive aeolian landforms of varying shape and size constructed from unconsolidated sand (Hugenholtz et al., 2012). Dunes are generally smaller in scale than mountains and this challenges our approach to basic-landform/relief classification mapping (Shumack et al., 2020), increasing the difficulty of accurate dune mapping. In this study, we regarded sand dunes as hills/low-relief rugged land/rugged terrain due to their morphological similarity. However, the variation of dune size and shape poses significant challenges to the accuracy of dune classification under the current unified framework. due to the variation of dune size and shape, it is challenging to correctly classify these dunes as hills according to our proposed method. Therefore, we design an optimization step to correct the classification results in which dunes and inter-dune areas are separated and identified according to their altitude and SRI. Firstly, on the basis of on their geomorphological characteristics, remote sensing images, and hillshade maps, we demarcated the major global sand desert regions. Secondly, we used the DEM to extract the topographic feature lines by surface

analysis of extracting desert feature lines. Employing the SURI calculation as for other regions, we then constructed the base terrain. In this case, the river-drainage networks were extracted with the threshold T_{D1} of 20000, and then we extracted sampling points from these networks to construct TINs. We calculated the SRI and then set the segmented threshold T_{D2} . Due to inconsistencies in the scale of dunes worldwide, we applied an adjustable T_{D2} ranging from 2m to 10m. Areas less than T_{D2} are defined as inter-dunes (equivalent to plains in the basic landform classification). All patches smaller than T_{D3} 0.02km^2 were regarded as fragments and integrated into the surrounding vector blocks. Finally, we employed the smoothing tool to ensure appropriateness of the landform boundary.

3 Results and discussion

3.1 Global landform-relief classification results



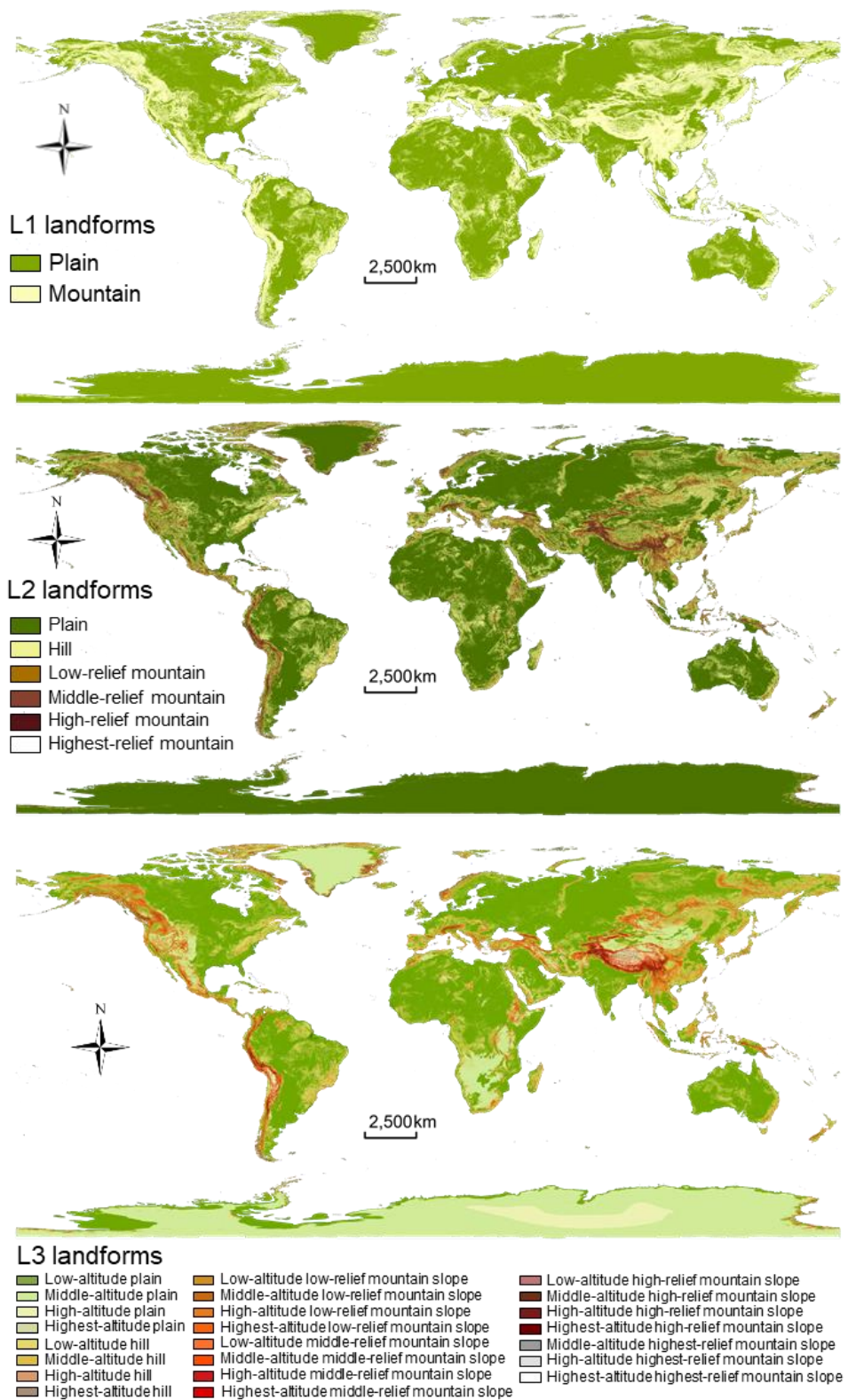
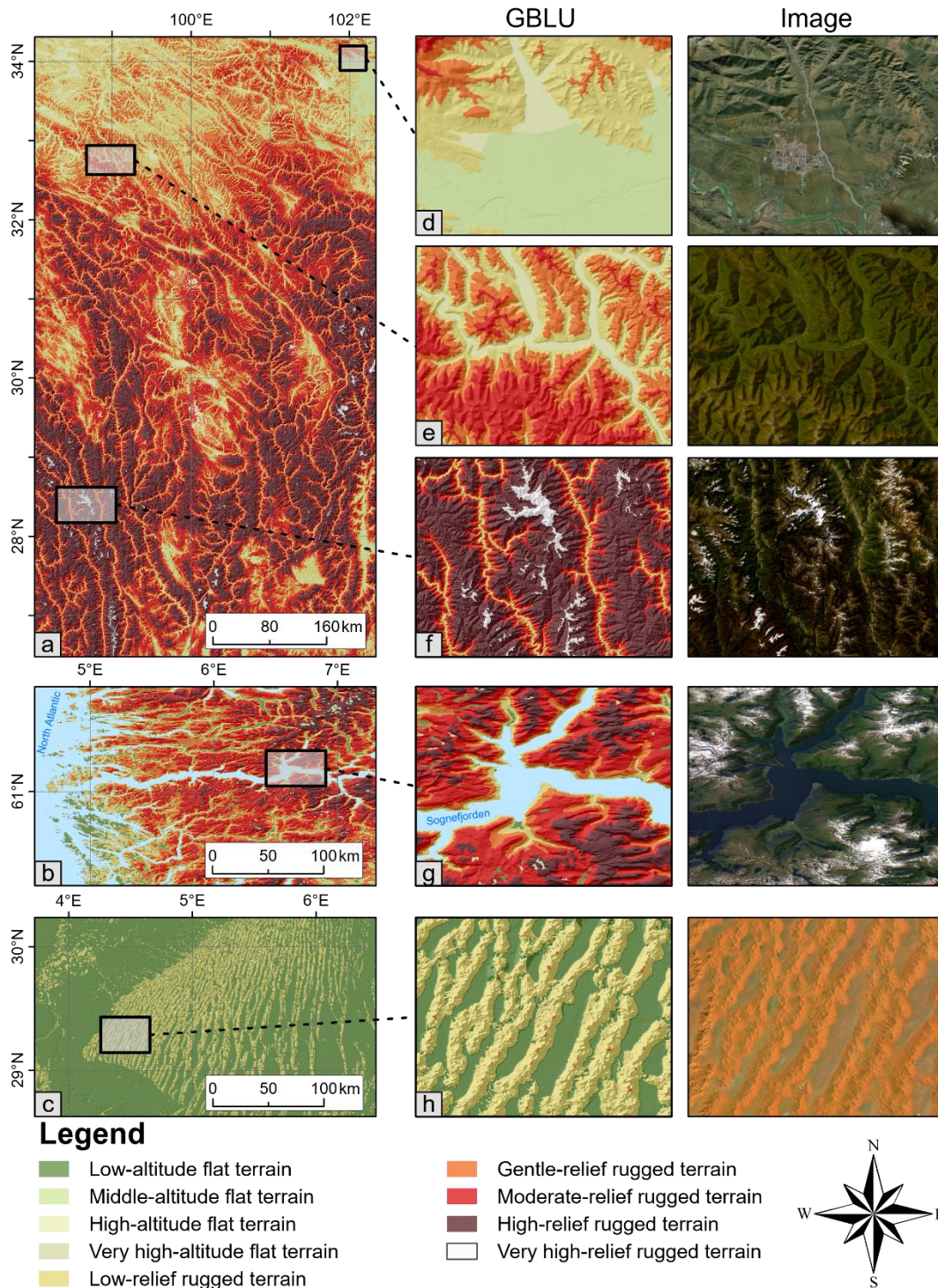


Figure 4. Results of the basic global landform/global relief classes classification—with 30 m resolution. **a**, **b** and **c** represent the L1, L2 and L3 landforms and L2 classes, respectively.

Figure 4 shows the global relief/global landform classification (GRC) results based on the abovementioned framework. This hierarchical dataset provides a more comprehensive understanding of the Earth's surface. To visualize the results in detail, three typical regions are selected to demonstrate the performance of the GBLUGRC dataset. Figure 5 shows the GBLUGRC in typical

regions and corresponding remote sensing image from Esri world imagery. The selected regions contain examples of the main ~~landforms~~ land surface on Earth, as well as transition areas of different ~~landforms~~ relief classes. In the mountainous areas, as shown in Figure 5a, ~~mountain~~ rugged land ~~rugged terrain~~ range and valley orientation are clearly discernible, which together form the fundamental structure for expressing mountains. The GBLUGRC clearly illustrates the transition zones between mountains (~~represented by the rugged land~~ rugged terrain) and plains (~~represented by the flat land~~ terrain), as well as potential floodplains. While such phenomena are visually discernible in remote sensing imagery, using our proposed framework, they are extracted based on quantified morphological characteristics. The abundant information on ~~the landform~~ landform composition provided by GBLUGRC can facilitate study of areas with high geomorphological value, such as fjords (Figure 5b). In desert areas Figure 5c, GBLUGRC effectively illustrates the transitional patterns between dunes and depressions. Based on abundant morphological characteristics, GBLUGRC can depict sand dune boundaries that are strikingly consistent with those visible in imagery. This further underscores ~~underscore~~ the performance of GBLUGRC in capturing detailed geomorphic features across varied terrains.



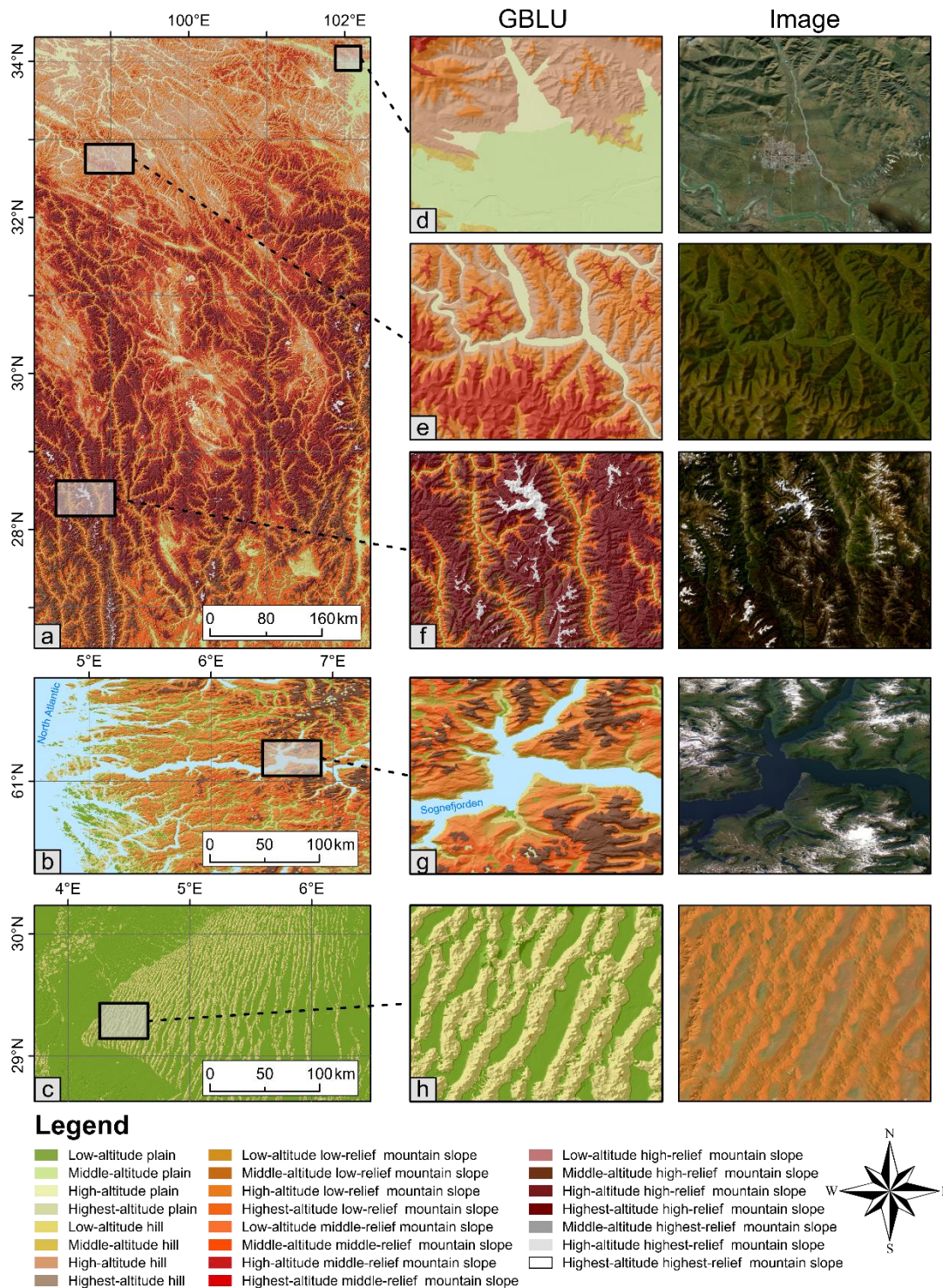
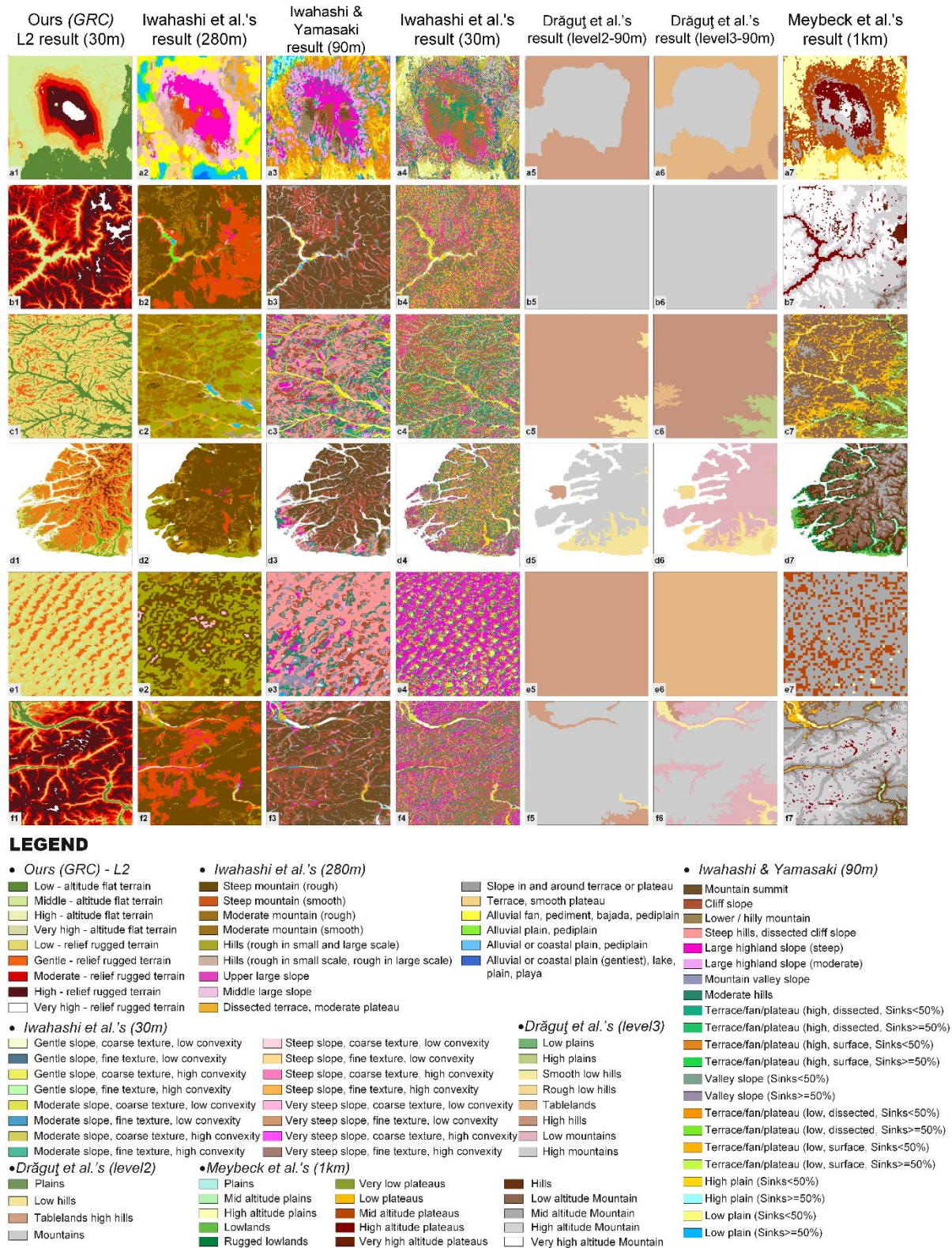


Figure 5. Comparison of landform the classification results constructed in this paper and remote sensing imagery. a eastern part of the Tibetan Plateau. **b** the Fjord coast in western Norway. **c** desert area in the central Sahara. **e-h** are local enlarged areas.



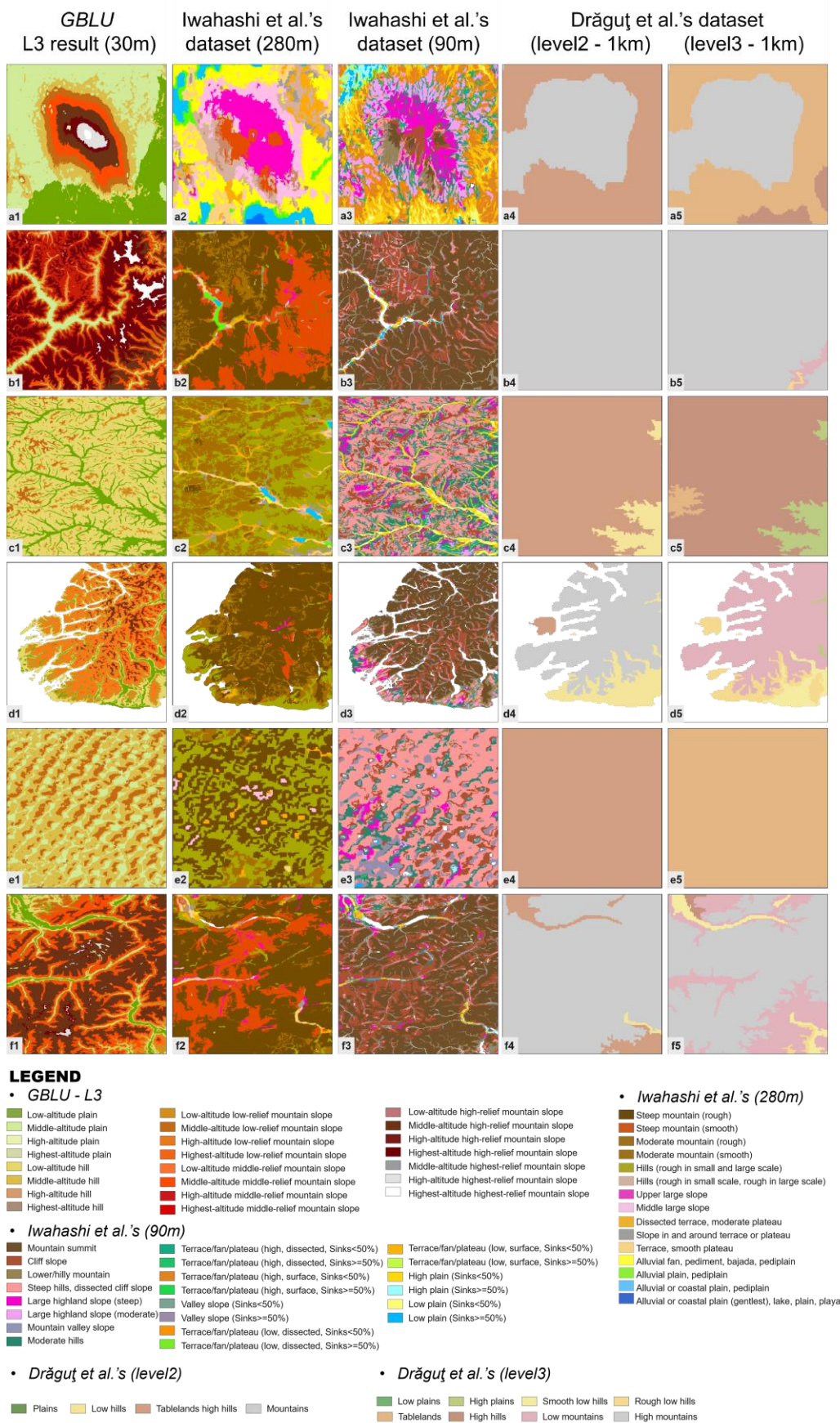


Figure 6. Comparison of GBLUGRC with other landform-classification results. Selected study areas, from top to bottom, are as follows: **a.** the Kilimanjaro, **b.** Namcha Barwa in Himalaya, **c.** Greater Khingan Mountains, **d.** Fjords in New Zealand, **e.** Badain Jaran Desert and **f.** Central Alps.

We conducted comparisons between the GBLUGRC dataset and multiple other datasets (including landform, terrain and relief classification) to comprehensively evaluate our results. ~~Specifically, we compared the outcomes of five landform classifications across a range of sample areas.~~ The most significant improvement achieved by applying GBLUGRC is the increased detail in representing terrain features. The GBLUGRC-based ~~landform~~ classification markedly enhances the delineation of independent landforms, such as dunes and mountains, which have clear boundaries and serve as key elements in the analysis of spatial structure and interactions. Meanwhile, ~~the~~ valley-like d objects can also be reflected by GBLUGRC. The classification systems of Drăguț and Blaschke (2006) are similar to GBLUGRC but have a coarser resolution of 1 km, making them less effective in capturing terrain details. Figure 6 illustrates that there is a variation in the understanding of landform types among different scholars. As noted above, Iwahashi's results align more closely with terrain classification systems in capturing slope features, such as flow channels on volcanic flanks, which occur at finer spatial scales than the terrain objects represented by GRCAs mentioned before, ~~Iwahashi's results align more closely with terrain classification systems. They represent a lot of slope details, such as flow channels on the volcanic slopes. In this paper, we consider landforms of plain or mountain to represent, which represent larger lower scales relative to terrain objects than GRC like "slope."~~ Therefore, in designing the classification system, we think that categorizing 'slope' at the same level as 'plain' or 'mountain' can lead to some comprehension difficulties. Therefore, GBLU offers a more comprehensive landform classification system and expresses the integrity of landform objects more closely aligned with the ontological understanding of landforms. It is worth noting that, as illustrated in Figure 6e, the incorporation of the SRI leads to the classification of dunes into three distinct sub-classes: ridge, slope, and interdune. While this finer-level classification provides enhanced information on relief variations, it may be perceived as compromising landform integrity in certain application contexts. Therefore, we recommend that users select either the L1 or L2 classification level depending on their specific research or application needs in desert areas.

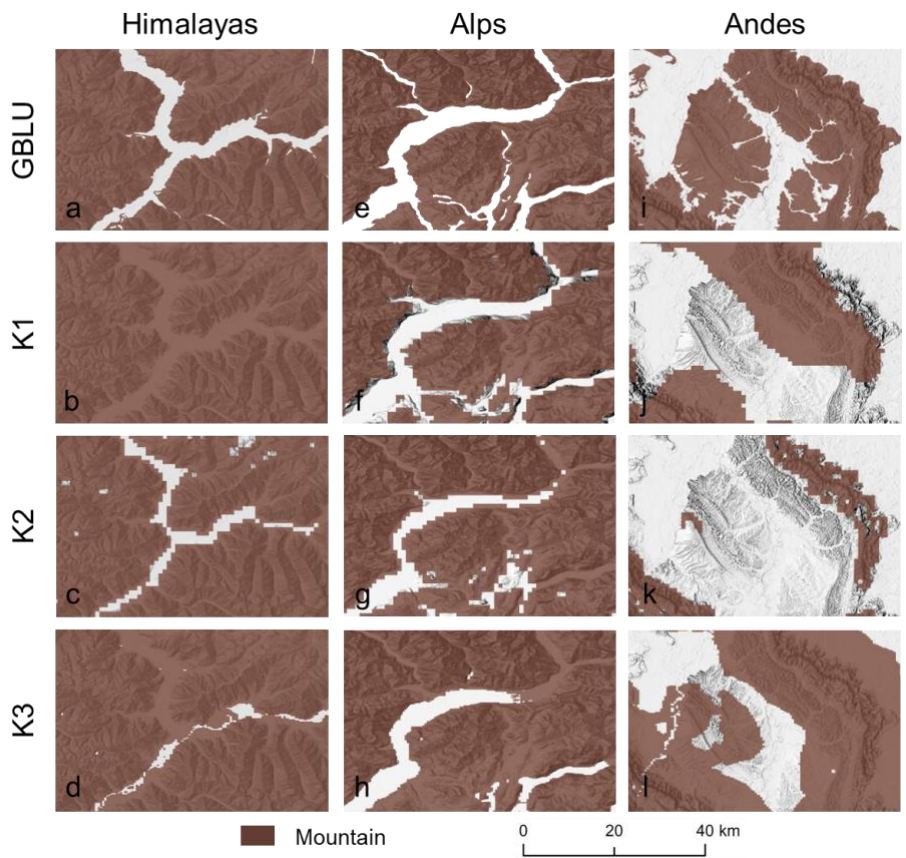
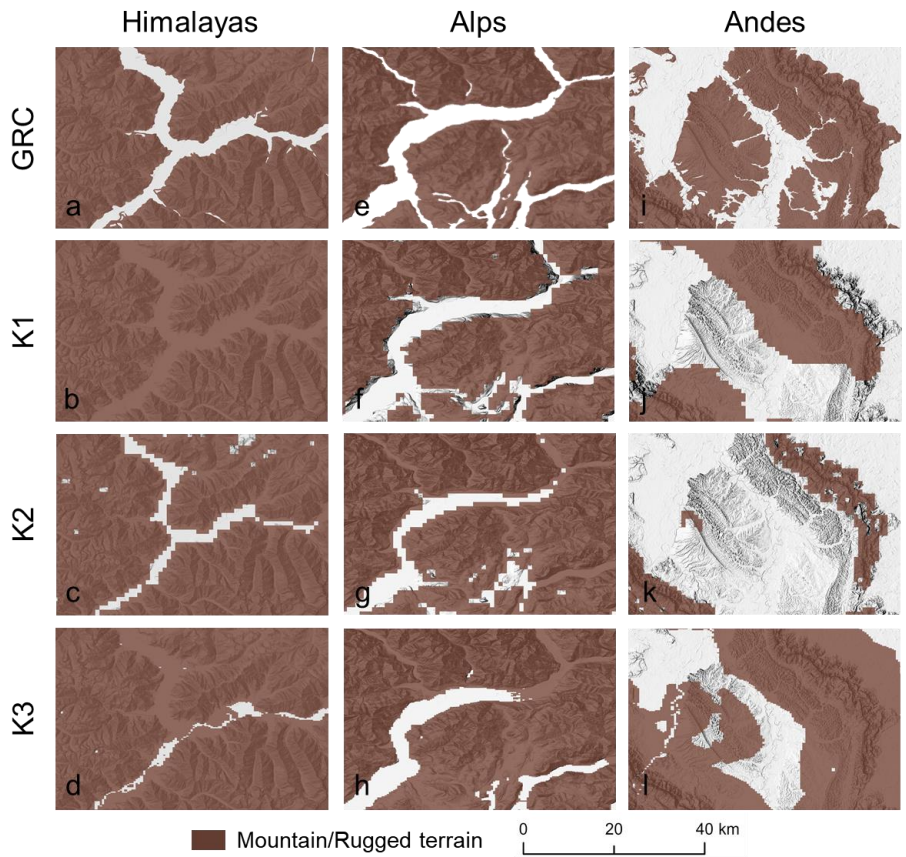


Figure 7. Comparison between the **GBLU****GRC** and three mountain definitions presented on the Global Mountain Explorer (<https://rmgsc.cr.usgs.gov/gme/>~~https://rmgsc.cr.usgs.gov/gme/~~).

We conducted a more detailed comparison ~~for of~~ mountain regions ~~with to reference from~~ the Global Mountain Explorer (GME) ~~as reference data~~. The GMBA-GME dataset contains three subsets using the DEM with spatial resolutions of 1000 m, 1000 m and 250 m to generate global mountain maps. These three datasets (e.g., K1, K2 and K3) are produced by analyzing the morphological derivatives, using a moving neighbourhood analysis window for ~~relief, elevation, and slope~~ derivative calculation (Kapos et al., 2000; Karagulle et al., 2017; Körner et al., 2011). Differences in application objectives and the selection of input variables have led to notable discrepancies among the classification results of the three datasets. K1 was established to support the global mapping of mountain forests by identifying mountainous regions where a combination of elevation, slope, and terrain ruggedness surpasses exceeds certain threshold values. K2, aimed at enabling comparative studies of mountain biodiversity, employed a comparable methodology but relied exclusively on ruggedness as the determining factor. Meanwhile, K3 emerged from efforts to construct a global ecosystem map, in which mountainous areas were defined by extracting this particular category from a broader classification of “ecological land units” (Sayre et al., 2018; Thornton et al., 2022). That similar indicators are used in the associated ~~classification and mapping processes indicates the comparability of the GMBA and the GBLU datasets, although due to differences in the category settings among the GBLU and the GMBA datasets, the comparison in this study focused only mountains.~~ As shown in Figure 7, the GBLUGRC dataset clearly outperforms the other three datasets in depicting mountain details, especially in representing valleys. This can be seen in Figures 7a-h, whereby the K1, K2 and K3 data exhibits separated upland blocks in mountainous regions with complex and intense terrain variations, and fails to represent continuous valleys.

~~Due to differences in classification systems and indices, it is challenging to conduct further quantitative comparisons between GBLU and other results. To facilitate comparison between these datasets, we merged some classes in the datasets to maintain classification consistency. For example, we merged mountain summit and cliff slope sections into ‘mountain’ as per merging criteria described in Table A2. Overall, GBLU results are consistent with other systems in terms of the macroscopic landform patterns. The merged results indicate that Iwahashi and Yamazaki's dataset performs better in representing plains boundaries and their shapes.~~

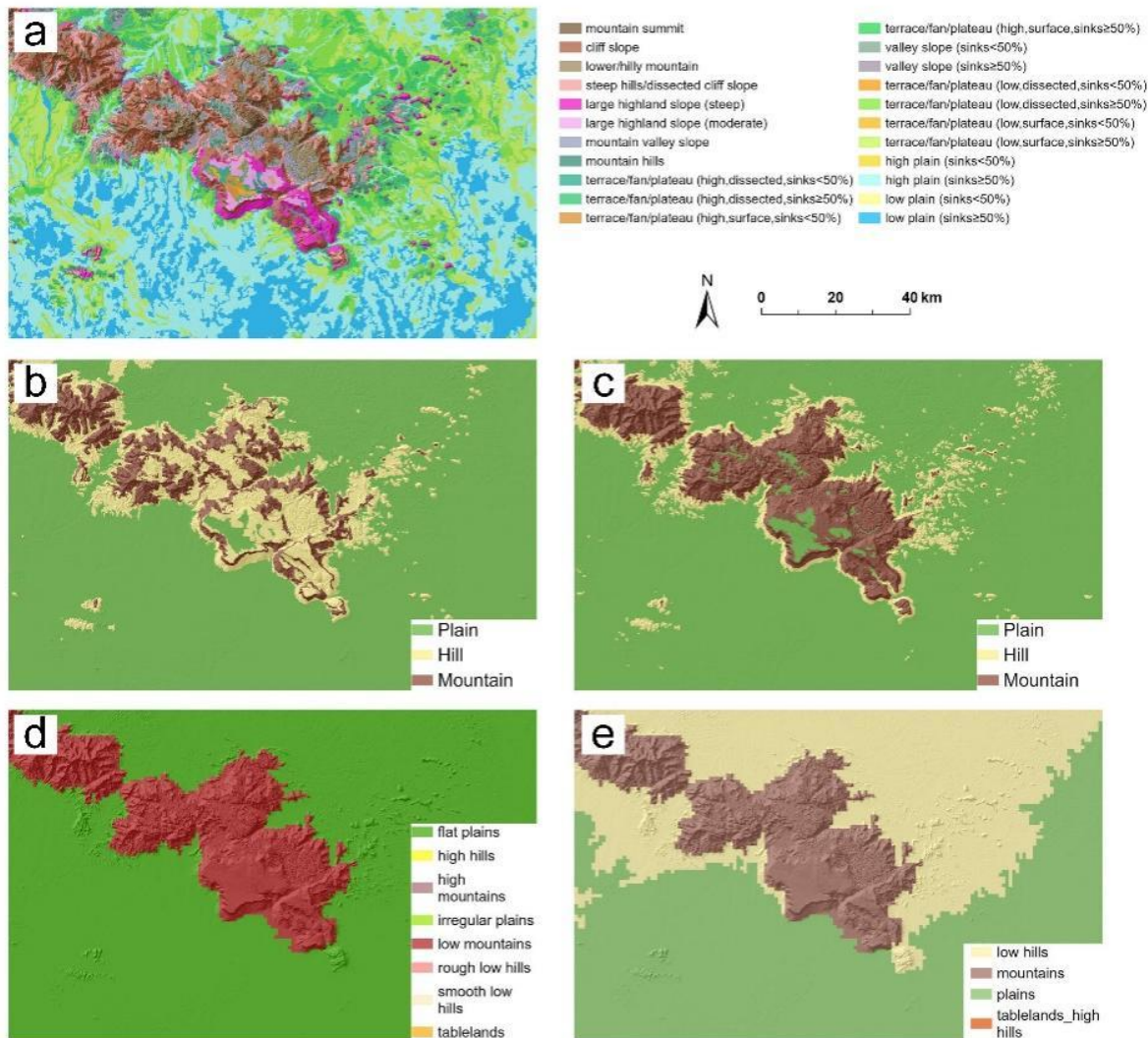
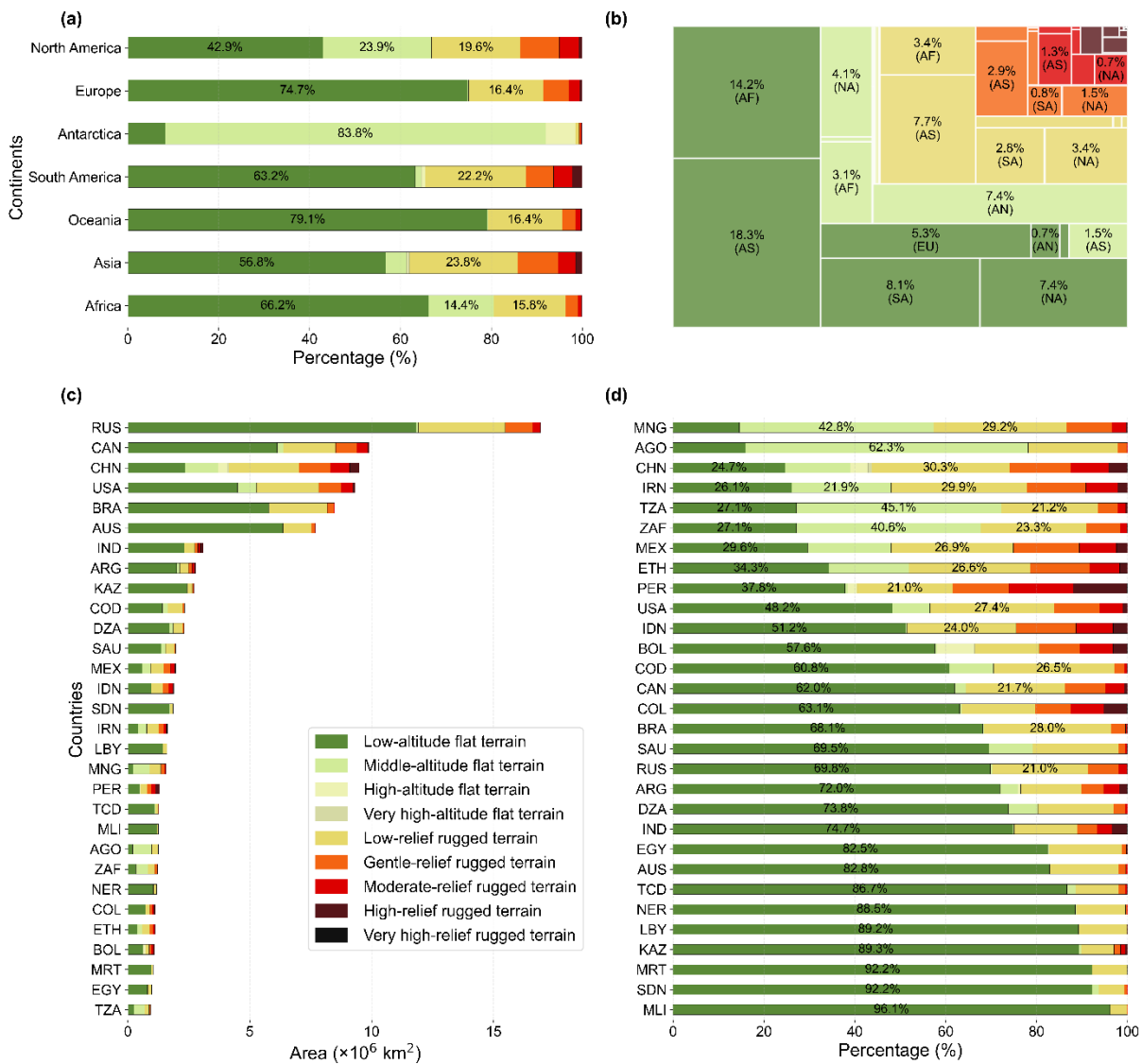


Figure 8. Classification result of the GBLU for an existing landform mapping dataset in the Amazon River basin.

a Iwahashi and Yamazaki (2022) original result; **b** adjusted Iwahashi and Yamazaki, 2022 result through merging landform classes; **c** GBLU result; **d** Drăguț and Eisank (2012) result (level 3); **e** Drăguț and Eisank, 2012 result (level 2).

3.4.3 Global landform compositionContinental and national composition of relief classes



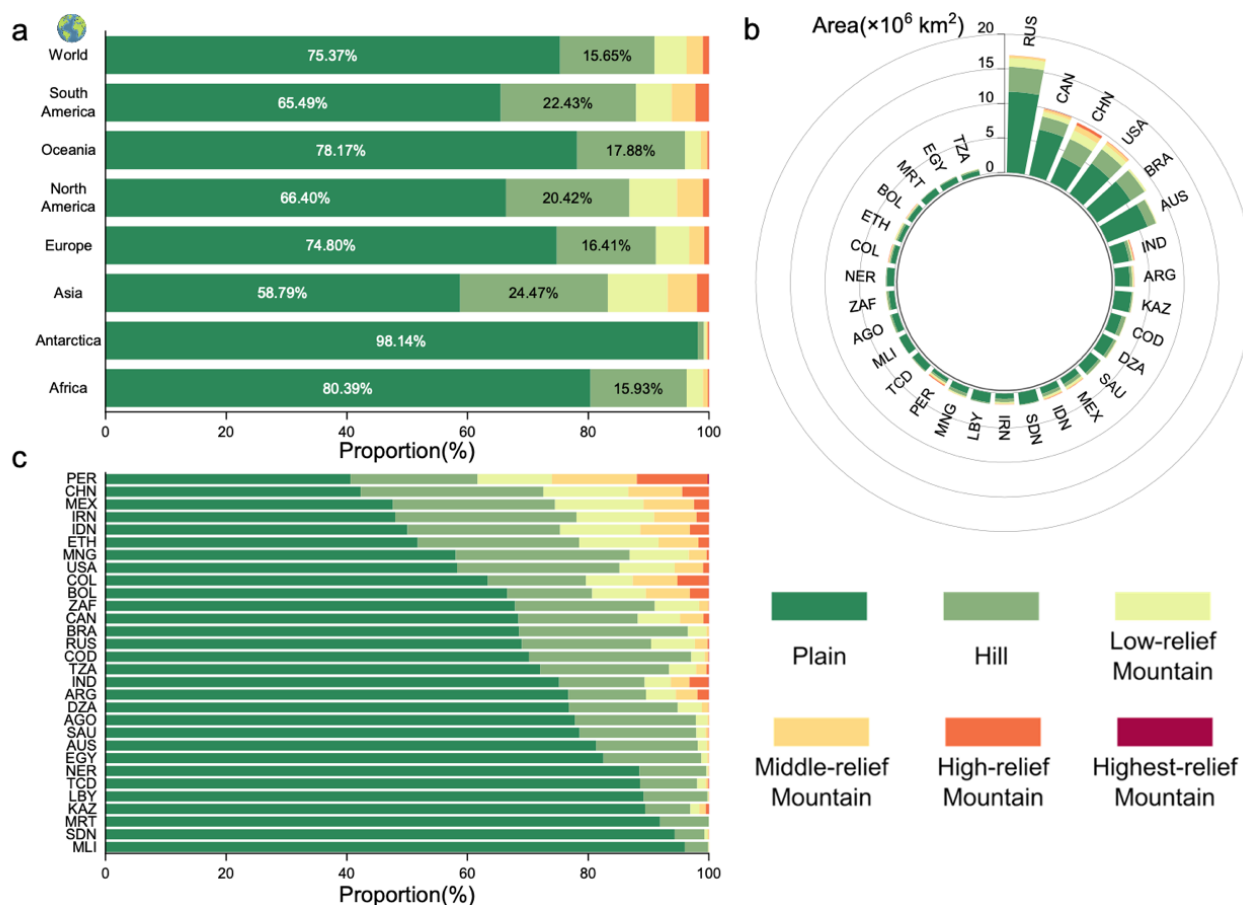


Figure 98. Area and proportional area statistics at continental and national scales. **a** Proportion of primary landformsGRC classes on each continent. **b** The square represents the proportion of each continent's relief types relative to the total global land area. A larger square indicates a-greater areas of that relief type for the continent. **b-c** Area of GRC classesprimary landform types in the top 30 countries ranked by area. **e-d** Proportion of GRC classesprimary landform types in the top 30 countries ranked by arealow-altitude flat landflat terrain. Full names of countries listed can be found in Table A3A2.

We have used a cell size of 500-100 m x 500-100 m to accurately assess the proportions of GRC L2 classes primary landforms across continents worldwide, thereby yielding insights into their spatial variations. We re-quantified the global distribution of relief classes and provides the most detailed estimates to date of the proportion of flat and rugged land terrain. The findings indicate that approximately 75% of the global land area comprises plain terrain, while some 16% consists of hills rugged terrain, with the remaining portion is classified as mountains rugged terrain (Figure 9a). In terms of the distribution of landform composition, Asia exhibits a very distinctive pattern, since plains the flat land flat terrain cover only 59% of its land area, the lowest among all continents, while there is a significantly higher proportion of hills and mountains rugged land terrain, consistent with its pronounced topographic diversity. Africa is characterized by the dominance of extensive flat lands terrain in terms of relative area. However, in absolute terms, Asia contains a significantly larger extent of flat land flat terrain, exceeding that of Africa by approximately 4.1%.

(Figure 8b). Compared to the global [averagescale](#), the presence of continental marginal mountain chains results in a significantly lower proportion of [plainsflat landterrains](#), and correspondingly higher proportion of [mountainsrugged landsterrain](#), in both North and South America. Indeed, South America has very substantial areas of high relief mountains, while Africa is distinguished by the dominance of extensive plains.

We further conducted a comprehensive analysis of [landform-relief classes types](#) and their proportions at the national and regional scale across all countries and regions worldwide to reveal patterns of variation. Figure [9b-8c](#) illustrates the proportion of [L2 classes-primary landform types](#) in the top 30 countries ranked by area, while Figure [9e-8d](#) depicts the standardized proportion of the [landform-relief classestypes](#) within these countries, sorted based on the proportion of [plainslow-altitude flat landflat terrain](#). China contains a significantly high proportion of rugged terrainlands, indicating its diverse and rugged landform composition, 's diverse and rugged topography is evident in its significantly high proportion of mountains, while Peru contains the lowest proportion of plainsflat lanterrains (40.5%), as mountainous terrain there occupies over 60% of its land area.

3.4 Geographic relationships: runoff, climate and land use Dataset usage note

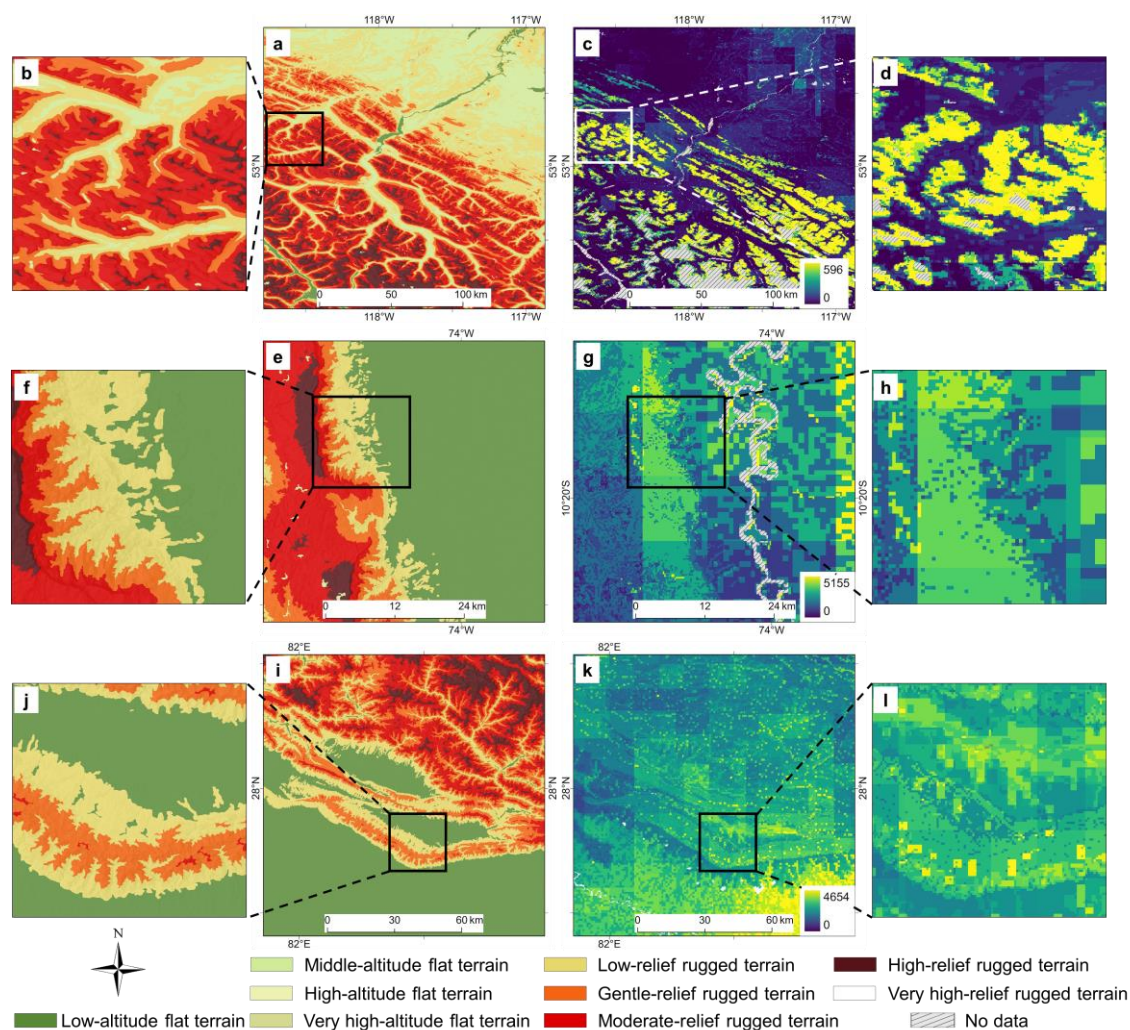
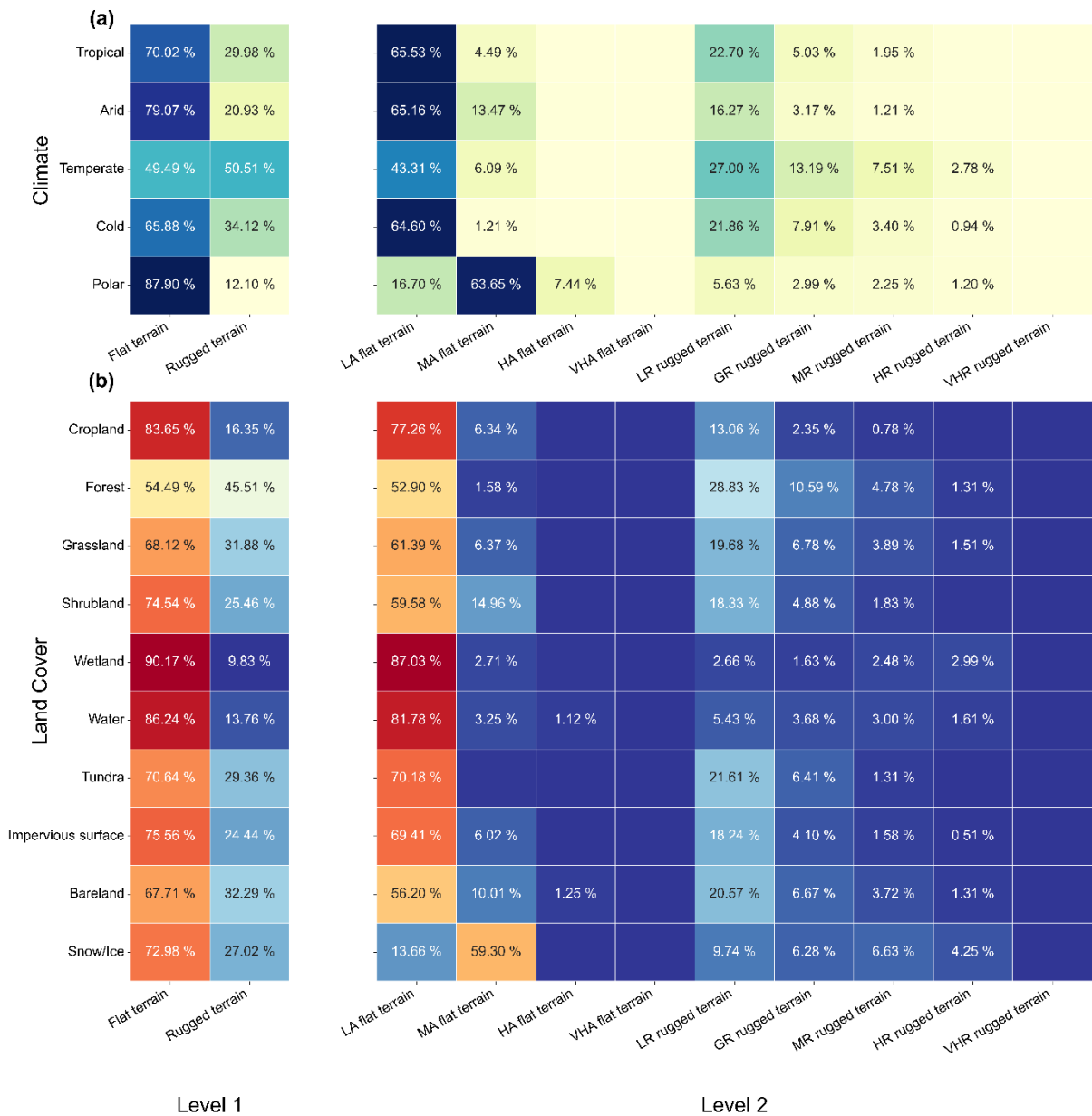


Figure 9. The spatial distribution of GRC and surface runoff in different areas. a and b show the GRC L2 for the Rocky Mountains in North America, while c and d display the corresponding runoff patterns in the same region. e and f show the GRC L2

for the Andes Mountains in South America, while **g** and **h** display the corresponding runoff patterns in the same region. **i** and **j** show the GRC L2 and runoff in the southern areas of the Himalayas, while **k** and **l** display the corresponding runoff patterns in the same region.

In this section, we highlight the results of experiments performed to ~~analyse~~analyze the relationships between ~~landforms~~relief classes, surface runoff, climate and land cover to highlight the potential applications of **GBLUGRC**. Based on the ~~high-high-~~resolution ~~landform-classes~~results provided by **GBLUGRC**, we can explore the complex and in-depth relationships between various factors~~landforms, climate, and land cover~~. Runoff data used in this study were obtained from GCN250 (Sujud and Jaafar, 2022), a global mean monthly runoff dataset for April 2015–2021 available in GeoTIFF format at a 250-meter resolution. This high-resolution dataset is valuable for a wide range of water-related applications, such as hydrologic design, land management, water resource allocation, and flood risk assessment. As shown in Figure 9 marked by red circles, we found that the spatial distribution of runoff closely aligns with the patterns represented by the GRC dataset. Notably, as shown in Figures 9e to l, substantial differences in runoff values are observed at the boundaries between flat and ~~rugged land~~rugged terrain, suggesting a strong association between runoff and terrain relief. This phenomenon indicates that the GRC data can help reveal such underlying spatial relationships. Moreover, in mountainous areas, the runoff values tend to follow valley-aligned patterns, which correspond well to the L2 classes in the GRC dataset. However, due to the coarse resolution of the GCN250, these gradual transitions are not fully captured. As a detailed representation of terrain relief, the GRC dataset holds potential for supporting downscaling of global runoff data. Integrating both datasets ~~could provide~~offers novel insights into surface water dynamics and improves our understanding of water resource management under complex topographic conditions. The climate data is the widely used 1-km Köppen-Geiger climate classification maps in 1991–2020 (Beck et al., 2023) and the land cover data is from FROM-GLC 30m in 2017 (Yu et al., 2013).



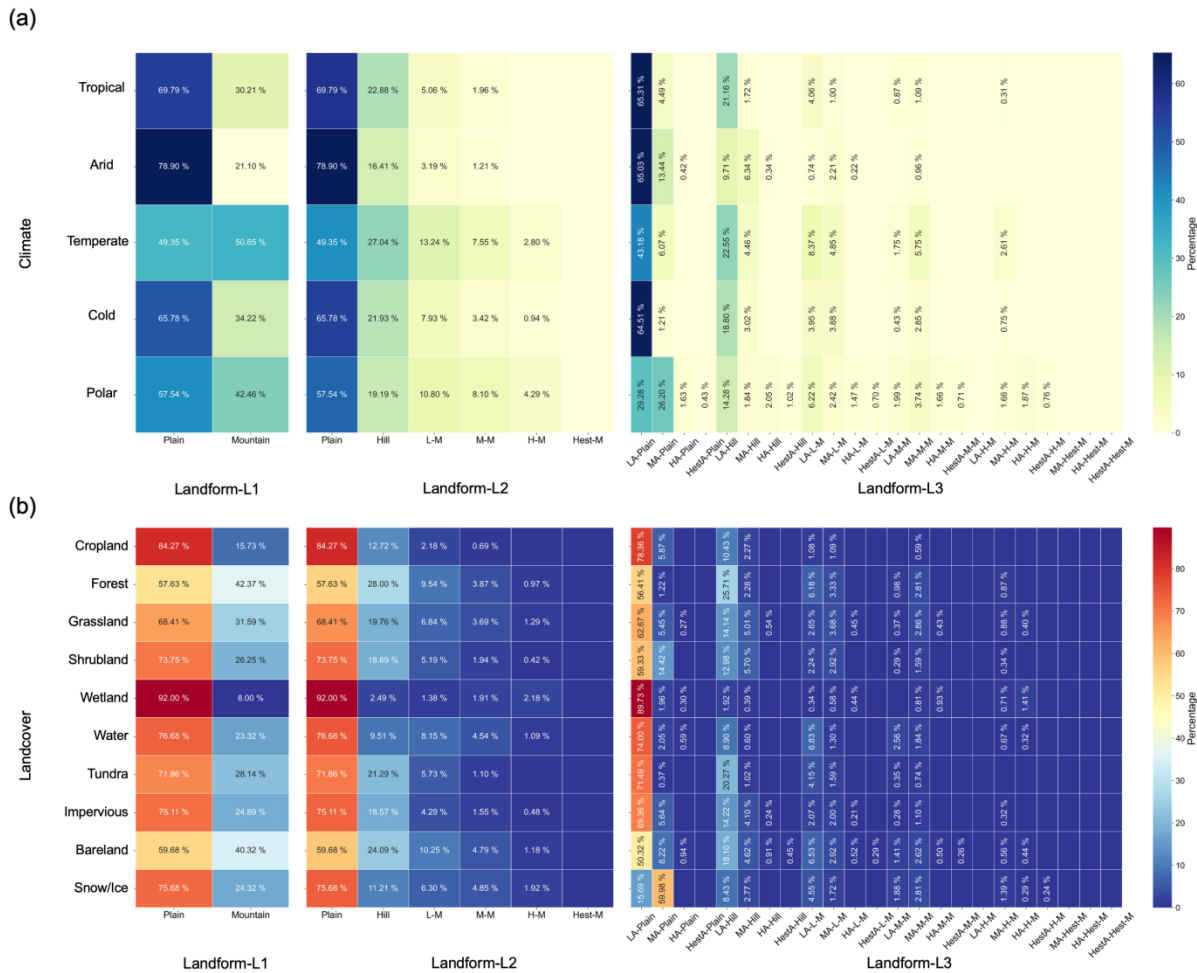


Figure 10. Relationship of landform types-relief classes to climate and land cover. (a) and (b) show the proportions of the three classes of landform types-relief class in different climatic and land cover regions respectively. Values less than 0.2% are not labeled with numbers. The climate data is the widely used classes as per the 1-km Köppen-Geiger climate classification maps for 1991–2020 (Beck et al., 2023); and the land cover data is from FROM-GLC 30m in 2017 (Yu et al., 2013). LA, MA, HA, VHA represent low-altitude, middle-altitude, high-altitude, very high-altitude, respectively. LR, GR, MR, HR, VHR represent low-relief, gentle-relief, moderate-relief, high-relief, very high-relief, respectively.

The enhanced resolution and detail of the GBLU enables subtle variations in the Earth's surface to be captured, which is highly valuable in understanding interactions between geomorphology and other factors. As shown in Figure 10, landform-relief class distribution in temperate zones suggests a unique blend of climatic conditions and geomorphologic land surface processes, fostering a diverse array of landforms-relief classes. In the climatic zones of tropical, arid, and cold regions, we observe that low-altitude plains-flat land and hills-low-relief rugged land are most prominent. A special case occurs in the polar regions, where a large share of the surface area is situated at higher altitudes compared to other climate zones. This pattern is primarily attributed to the extensive presence occurrence of ice sheets, which substantially elevate surface elevation and modify the observed relief patterns in these regions. For polar areas, a larger proportion of the area is located at higher altitudes than in other

~~climate zones~~. Regarding land cover analysis (excluding the South Polar area), cropland occupies ~~8483.2765%~~ of ~~plains-flat land~~ ~~flat terrain~~ and ~~1516.7335%~~ of ~~mountains~~ ~~rugged land~~ ~~rugged terrain~~, yielding useful insights for analyzing cultivated land productivity. Meanwhile, forests and bare land are more prevalent in ~~mountains~~ ~~moderately to highly rugged land~~ ~~rugged terrain~~, ~~more~~ especially in ~~hills~~ ~~low-relief areas~~. Additionally, the percentage of many ecologically significant biomes, such as forests, grasslands, wetlands, tundra, and water bodies, in ~~plains-flat~~ and ~~mountainous-rugged~~ regions has been brought up to date. This is potentially valuable for assessing the quality of ecological environments and carbon stocks.

The ~~GBLUGRC~~ provided in this work has obvious applications in geomorphology but also in other fields and can, moreover, play a fundamental role in supporting the identification of landforms that incorporates domain background. For example, identification of a landscape element as ‘tableland’ is complex, differs between disciplines, and requires that both morphological and evolutionary characteristics be accounted for. The ~~GBLUGRC~~ can be integrated with additional observations to map the occurrence and distribution of tablelands through the delineation of segments that are elevated, flat, and surrounded by steep escarpments. There is also significant potential for the application of ~~GBLUGRC~~ to other fields (such as geology, hydrology and ecology) focusing on the natural environment. For example, for ecologists, biodiversity distribution across different landform regions is one of the most significant issues and central to understanding the nature of ecosystem change. At the regional scale, contrasting geomorphological conditions are known to promote isolation of biological populations, influencing community structure and function, as well as evolution. Meanwhile, the interaction between geomorphology and biogeography may result in complex bio-geomorphological dynamics. The feedback between physical, ecological and evolutionary components constituting bio-geomorphological systems is an important element of the evolution of the Earth's surface.

4. Dataset access

~~Global relief classification-(GRC-v1.0) data is stored in the Deep-time Digital Earth Geomorphology platform and Zenodo (Yang et al., 2024; <https://doi.org/10.5281/zenodo.15641257>). We employed a 1° x 1° grid to tile the data for storage, with 25,252 file tiles in all. We distinguish the types of landform units by coding attributes of the elements. Additionally, we provide a rasterized dataset (at 30m resolution) using the coordinate system of WGS84 Web Mercator. Values of the cells represent the codes of L2 types. Meanwhile, in order to further the application, we also stored data in Esri shapefile format using the coordinate system WGS84. Total size of the dataset is 150GB. In the attribute table, field “code 1” is the landform type code of the first level L1, field “code 2” is the landform type code of the sub-level L2.~~ Global Basic Landform Units (GBLU-v1.0) is stored in the Deep-time Digital Earth Geomorphology platform and Zenodo (Yang et al., 2024; <https://doi.org/10.5281/zenodo.13187969>). The data are stored in Esri shapefile format using the coordinate system WGS84. Total size of the dataset is 150GB, with 6,849,306 independent landform blocks. In order to facilitate application, we employed a 1° × 1° grid to tile the data for storage, with 25,252 file tiles in all. We distinguish the types of landform units by coding attributes of the elements. Additionally, we provide a rasterized dataset (at 30m resolution) using the coordinate system of WGS84. Values of the cells represent the codes of L3 types. In the attribute table, field

~~“code0” is the landform type code of the first level, field “code1” is the landform type code of the second level and field “code2” is the landform type code of the L3.~~

5. Conclusion

This study provides a novel global ~~landform-relief~~ classification ~~dataset (GBLU)-dataset~~ with a resolution of 1 arc-second (approximately 30 m). In this study, we propose a ~~novel~~ framework for global ~~landform-land surface~~ mapping to significantly improve the quantitative evaluation of ~~geomorphological-topographic~~ features. The key output is the release of the GBLUGRC dataset that is suited to applications across multiple disciplines, including geography, geology, ecology, and hydrology. Global-scale analysis of attributes within the GBLUGRC reveals the composition and distribution of global landforms that enables comparison between regions and continents. The results emphasize the notable heterogeneity of Asia in general, and of China in particular, in terms of ~~geomorphological-relief~~ diversity. The GBLUGRC outperforms previous datasets in expressing ~~landform-object~~ details, providing an opportunity to investigate the Earth’s natural resources. The resolution of the GBLUGRC is similar to that of the current mainstream remote sensing data, which makes combined use of the data relatively simple. We believe that this dataset can provide abundant and detailed geomorphological information for the field of earth sciences, facilitating further advancements in related research.

Appendix A

Table A1. Classification of global basic landform-relief types

<u>L1</u>	<u>Code1</u>	<u>Colors (RGB)</u>	<u>L2</u>	<u>Code2</u>	<u>Colors (RGB)</u>	<u>Note</u>		
<u>Flat land</u> <u>Flat terrain</u>	<u>1</u>	<u>129,168,0</u>	<u>Low-altitude flat land</u> <u>flat terrain</u>	<u>11</u>	<u>90,138,55</u>	<u>Classifying L2 flat lad based on the altitude.</u>		
			<u>Middle-altitude flat land</u> <u>flat terrain</u>	<u>12</u>	<u>209,235,152</u>			
			<u>High-altitude flat land</u> <u>flat terrain</u>	<u>13</u>	<u>237,242,179</u>			
			<u>Highest-altitude flat land</u> <u>flat terrain</u>	<u>14</u>	<u>213,217,164</u>			
<u>Rugged land</u> <u>Rugged terrain</u>	<u>2</u>	<u>255,255,190</u>	<u>Low-relief rugged land</u> <u>rugged terrain</u>	<u>21</u>	<u>230,216,106</u>	<u>Classifying L2 rugged lad based on the surface relief index.</u>		
			<u>Gentle-relief rugged land</u> <u>rugged terrain</u>	<u>22</u>	<u>244,100,18</u>			
			<u>Moderate-relief rugged land</u> <u>rugged terrain</u>	<u>23</u>	<u>220,0,0</u>			
			<u>High-relief rugged land</u> <u>rugged terrain</u>	<u>24</u>	<u>86,20,24</u>			
			<u>Very high-relief rugged land</u> <u>rugged terrain</u>	<u>25</u>	<u>255,255,255</u>			
<u>L1</u>	<u>Code</u>	<u>Colors (RGB)</u>	<u>L2</u>	<u>Code</u>	<u>Colors (RGB)</u>	<u>L3</u>	<u>Code</u>	<u>Colors (RGB)</u>
<u>Plain</u>	<u>4</u>	<u>129,168,0</u>	<u>Plain</u>	<u>44</u>	<u>76,115,0</u>	<u>Low-altitude plain</u>	<u>441</u>	<u>112,168,0</u>
						<u>Middle-altitude plain</u>	<u>442</u>	<u>209,235,152</u>
						<u>High-altitude plain</u>	<u>443</u>	<u>237,242,179</u>


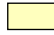
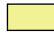


















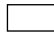


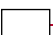
						Highest-altitude plain	114		213,217,164		
Mountain	2		255,255,190	Hill	21		240,242,148	Low-altitude hill	211		230,216,106
								Middle-altitude hill	212		220,191,75
								High-altitude hill	213		217,155,110
								Highest-altitude hill	214		170,141,117
								Low-relief Mountain	22		168,112,0
				Middle-altitude low-relief mountain-slope	222		198,106,20				
				High-altitude low-relief mountain-slope	223		237,122,24				
				Highest-altitude low-relief mountain-slope	224		244,100,18				
				Middle-relief Mountain	23		137,65,47	Low-altitude middle-relief mountain-slope	231		253,120,25
								Middle-altitude middle-relief mountain-slope	232		255,76,0
								High-altitude middle-relief mountain-slope	233		201,30,9
								Highest-altitude middle-relief mountain-slope	234		220,0,0
				High-relief Mountain	24		86,20,24	Low-altitude high-relief mountain-slope	241		193,119,120
								Middle-altitude high-relief mountain-slope	242		110,50,20
								High-altitude high-relief mountain-slope	243		114,4,9
								Highest-altitude high-relief mountain-slope	244		115,0,0
				Highest-relief Mountain	25		255,255,255	Middle-altitude highest-relief mountain-slope	252		156,156,156
								High-altitude highest-relief mountain-slope	253		225,225,225
								Highest-altitude highest-relief mountain-slope	254		255,255,255

Table A2. Merging the GBLU results to enable comparison with the results of Iwahashi and Yamazaki.

	Terrain22	Gcluster15	Sinks	legend
Mountain	1	2	1,0	Mountain summit
	2	3	1,0	Cliff slope
	3	13	1,0	Lower/hilly mountain
	4	12	1,0	Steep hills/dissected cliff slope
	5	5	1,0	Large highland slope (steep)
	6	4	1,0	Large highland slope (moderate)
	7	14	1,0	Mountain valley slope
	8	10	1,0	Moderate hills
Hill	9*	11	0	Terrace/fan/plateau (high, dissected, Sinks < 50%)
	10	11	1	Terrace/fan/plateau (high, dissected, Sinks ≥ 50%)
	11	7	0	Terrace/fan/plateau (high, surface, Sinks < 50%)
	12	7	1	Terrace/fan/plateau (high, surface, Sinks ≥ 50%)
	13*	8	0	Valley slope (Sinks < 50%)
	14	8	1	Valley slope (Sinks ≥ 50%)
Plain	15*	9	0	Terrace/fan/plateau (low, dissected, Sinks < 50%)
	16	9	1	Terrace/fan/plateau (low, dissected, Sinks ≥ 50%)
	17*	6	0	Terrace/fan/plateau (low, surface, Sinks < 50%)
	18	6	1	Terrace/fan/plateau (low, surface, Sinks ≥ 50%)
	19*	1	0	High plain (Sinks < 50%)
	20	1	1	High plain (Sinks ≥ 50%)
	21*	15	0	Low plain (Sinks < 50%)
	22	15	1	Low plain (Sinks ≥ 50%)

Table A2. Countries' names and their abbreviations.

Abbreviations	Name
AGO	Angola
ARG	Argentina
AUS	Australia
BOL	Bolivia
BRA	Brazil
CAN	Canada
CHN	China
COD	Congo (Democratic Republic)
COL	Colombia
DZA	Algeria
EGY	Egypt
ETH	Ethiopia
IDN	Indonesia
IND	India
IRN	Iran
KAZ	Kazakhstan
LBY	Libya
MEX	Mexico
MLI	Mali
MNG	Mongolia
MRT	Mauritania
NER	Niger
PER	Peru
RUS	Russia
SAU	Saudi Arabia
SDN	Sudan
TCD	Chad
TZA	Tanzania
USA	United States <u>of America</u>

Author contribution

~~Xin-YangXY~~, ~~Guoan-TangGT~~ and ~~Michael-MeadowsMM~~ designed the study.

~~Xin-YangXY~~, ~~Sijin-LiSL~~, ~~Junfei-MaM~~, ~~Yang-ChenC~~ and ~~Xingyu-ZhouZ~~ performed the analysis.

~~Xin-YangY~~ and ~~Sijin-LiL~~ wrote the first version of the manuscript.

~~Fayuan-Li~~, ~~Liyang-Xiong~~ and ~~Chenghu-Zhou~~ coordinated the work and reviewed the manuscript.

~~Sijin-Li~~, ~~Junfei-Ma~~, ~~Yang-Chen~~ and ~~Xingyu-Zhou~~ assisted with quality control and reviewed the manuscript.

All the authors contributed to the final version of the manuscript.

Acknowledgment

The authors express their sincere gratitude to the journal editor and reviewers for their thoughtful suggestions, which have greatly contributed to improving the quality of this manuscript. Sincere thanks are also extended to many others for their valuable comments on this manuscript.

Competing interests

The authors declare that they have no conflict of interest.

Financial support

This study is supported by the National Natural Science Foundation of China (42171402; 42401507) and the Deep-time Digital Earth (DDE) Big Science Program.

References

- Amatulli, G., Domisch, S., Tuanmu, M.-N., Parmentier, B., Ranipeta, A., Malczyk, J., and Jetz, W.: A suite of global, cross-scale topographic variables for environmental and biodiversity modeling, *Sci Data*, 5, 180040, <https://doi.org/10.1038/sdata.2018.40>, 2018.
- Amatulli, G., McInerney, D., Sethi, T., Strobl, P., and Domisch, S.: Geomorpho90m, empirical evaluation and accuracy assessment of global high-resolution geomorphometric layers, *Sci Data*, 7, 162, <https://doi.org/10.1038/s41597-020-0479-6>, 2020.
- Beck, H. E., McVicar, T. R., Vergopolan, N., Berg, A., Lutsko, N. J., Dufour, A., Zeng, Z., Jiang, X., van Dijk, A. I., and Miralles, D. G.: High-resolution (1 km) Köppen-Geiger maps for 1901–2099 based on constrained CMIP6 projections, *Scientific data*, 10, 724, <https://doi.org/10.1038/s41597-023-02549-6>, 2023.
- Drăguț, L. and Blaschke, T.: Automated classification of landform elements using object-based image analysis, *Geomorphology*, 81, 330–344, <https://doi.org/10.1016/j.geomorph.2006.04.013>, 2006.
- Drăguț, L. and Eisank, C.: Object representations at multiple scales from digital elevation models, *Geomorphology*, 129, 183–189, <https://doi.org/10.1016/j.geomorph.2011.03.003>, 2011.
- Drăguț, L. and Eisank, C.: Automated object-based classification of topography from SRTM data, *Geomorphology*, 141–142, 21–33, <https://doi.org/10.1016/j.geomorph.2011.12.001>, 2012.
- Dramis, F.: Geomorphological mapping for a sustainable development, *Journal of Maps*, 1, 53–55, <https://doi.org/10.4113/jom.2009.1084>, 2009.
- Dyba, K. and Jasiewicz, J.: Toward geomorphometry of plains-Country-level unsupervised classification of low-relief areas (Poland), *Geomorphology*, 413, 108373, <https://doi.org/10.1016/j.geomorph.2022.108373>, 2022.

- Evans, I. S.: Geomorphometry and landform mapping: What is a landform?, *Geomorphology*, 137, 94–106, <https://doi.org/10.1016/j.geomorph.2010.09.029>, 2012.
- Florinsky, I. V.: An illustrated introduction to general geomorphometry, *Progress in Physical Geography: Earth and Environment*, 41, 723–752, <https://doi.org/10.1177/0309133317733667>, 2017.
- Gallant, A. L., Brown, D. D., and Hoffer, R. M.: Automated mapping of Hammond’s landforms, *IEEE geoscience and remote sensing letters*, 2, 384–388, <https://doi.org/10.1109/LGRS.2005.848529>, 2005.
- Hammond, E. H.: Small-Scale Continental Landform Maps, *Annals of the Association of American Geographers*, 44, 33–42, <https://doi.org/10.1080/00045605409352120>, 1954.
- Hawker, L., Uhe, P., Paulo, L., Sosa, J., Savage, J., Sampson, C., and Neal, J.: A 30 m global map of elevation with forests and buildings removed, *Environ. Res. Lett.*, 17, 024016, <https://doi.org/10.1088/1748-9326/ac4d4f>, 2022.
- Howat, I., Porter, C., Smith, B.E., Noh, M.J. and Morin, P.: The Reference Elevation Model of Antarctica – Strips, Version 4.1, Harvard Dataverse [data set], <https://doi.org/10.7910/DVN/X7NDNY>, 2022
- Hugenholtz, C. H., Levin, N., Barchyn, T. E., and Baddock, M. C.: Remote sensing and spatial analysis of aeolian sand dunes: A review and outlook, *Earth-Science Reviews*, 111, 319–334, <https://doi.org/10.1016/j.earscirev.2011.11.006>, 2012.
- Iwahashi, J. and Pike, R. J.: Automated classifications of topography from DEMs by an unsupervised nested-means algorithm and a three-part geometric signature, *Geomorphology*, 86, 409–440, 2007.
- Iwahashi, J. and Yamazaki, D.: Global polygons for terrain classification divided into uniform slopes and basins, *Prog Earth Planet Sci*, 9, 33, <https://doi.org/10.1186/s40645-022-00487-2>, 2022.
- Iwahashi, J., Kamiya, I., Matsuoka, M., and Yamazaki, D.: Global terrain classification using 280 m DEMs: segmentation, clustering, and reclassification, *Prog Earth Planet Sci*, 5, 1, <https://doi.org/10.1186/s40645-017-0157-2>, 2018.
- Jasiewicz, J. and Stepinski, T. F.: Geomorphons — a pattern recognition approach to classification and mapping of landforms, *Geomorphology*, 182, 147–156, <https://doi.org/10.1016/j.geomorph.2012.11.005>, 2013.
- Kapos, V., Rhind, J., Edwards, M., Price, M., Ravilious, C., and Butt, N.: Developing a map of the world’s mountain forests., *Forests in sustainable mountain development: a state of knowledge report for 2000*, Task Force For. Sustain. Mt. Dev., 4–19, <https://doi.org/10.1079/9780851994468.0004>, 2000.
- Karagulle, D., Frye, C., Sayre, R., Breyer, S., Aniello, P., Vaughan, R., and Wright, D.: Modeling global Hammond landform regions from 250-m elevation data, *Transactions in GIS*, 21, 1040–1060, <https://doi.org/10.1111/tgis.12265>, 2017.
- Körner, C., Paulsen, J., and Spehn, E. M.: A definition of mountains and their bioclimatic belts for global comparisons of biodiversity data, *Alp Botany*, 121, 73–78, <https://doi.org/10.1007/s00035-011-0094-4>, 2011.
- Li, S., Xiong, L., Tang, G., and Strobl, J.: Deep learning-based approach for landform classification from integrated data sources of digital elevation model and imagery, *Geomorphology*, 354, 107045, <https://doi.org/10.1016/j.geomorph.2020.107045>, 2020.
- Li, S., Xiong, L., Hu, G., Dang, W., Tang, G., and Strobl, J.: Extracting check dam areas from high-resolution imagery based on the integration of object-based image analysis and deep learning, *Land Degrad Dev*, 32, 2303–2317, <https://doi.org/10.1002/ldr.3908>, 2021.
- MacMillan, R. A. and Shary, P. A.: Landforms and landform elements in geomorphometry, *Developments in soil science*, 33, 227–254, [https://doi.org/10.1016/S0166-2481\(08\)00009-3](https://doi.org/10.1016/S0166-2481(08)00009-3), 2009.
- Martins, F. M. G., Fernandez, H. M., Isidoro, J. M. G. P., Jordán, A., and Zavala, L.: Classification of landforms in Southern Portugal (Ria Formosa Basin), *Journal of Maps*, 12, 422–430, <https://doi.org/10.1080/17445647.2015.1035346>, 2016.
- Maxwell, A. E. and Shobe, C. M.: Land-surface parameters for spatial predictive mapping and modeling, *Earth-Science Reviews*, 226, 103944, <https://doi.org/10.1016/j.earscirev.2022.103944>, 2022.
- Meybeck, M., Green, P., and Vörösmarty, C.: A new typology for mountains and other relief classes. *Mountain research and development*, 21(1), [https://doi.org/10.1659/0276-4741\(2001\)021\[0034:ANTFMA\]2.0.CO;2](https://doi.org/10.1659/0276-4741(2001)021[0034:ANTFMA]2.0.CO;2), 2001
- Pennock, D. J., Zebarth, B. J., and De Jong, E.: Landform classification and soil distribution in hummocky terrain, Saskatchewan, Canada, *Geoderma*, 40, 297–315, [https://doi.org/10.1016/0016-7061\(87\)90040-1](https://doi.org/10.1016/0016-7061(87)90040-1), 1987.
- Pepin, N.C., Arnone, E., Gobiet, A., Haslinger, K., Kotlarski, S., Notarnicola, C., Palazzi, E., Seibert, P., Serafin, S., Schöner, W. and Terzago, S.: Climate changes and their elevational patterns in the mountains of the world. *Reviews of geophysics*, 60(1), [p.e2020RG000730](https://doi.org/10.1029/2020RG000730), <https://doi.org/10.1029/2020RG000730>, 2022.

- Sayre, R., Frye, C., Karagulle, D., Krauer, J., Breyer, S., Aniello, P., Wright, D.J., Payne, D., Adler, C., Warner, H. and VanSistine, D.P.: A New High-Resolution Map of World Mountains and an Online Tool for Visualizing and Comparing Characterizations of Global Mountain Distributions. *Mountain Research and Development*, 38(3):240–249. <https://doi.org/10.1659/MRD-JOURNAL-D-17-00107.1>, 2018.
- Shumack, S., Hesse, P., and Farebrother, W.: Deep learning for dune pattern mapping with the AW3D30 global surface model, *Earth Surface Processes and Landforms*, 45, 2417–2431, <https://doi.org/10.1002/esp.4888>, 2020.
- Smith, B. and Mark, D. M.: Geographical categories: an ontological investigation, *International Journal of Geographical Information Science*, 15, 591–612, <https://doi.org/10.1080/13658810110061199>, 2001.
- Smith, B. and Mark, D. M.: Do Mountains Exist? Towards an Ontology of Landforms, *Environ Plann B Plann Des*, 30, 411–427, <https://doi.org/10.1068/b12821>, 2003.
- Snethlage, M. A., Geschke, J., Ranipeta, A., Jetz, W., Yoccoz, N. G., Körner, C., Spehn, E. M., Fischer, M., and Urbach, D.: A hierarchical inventory of the world's mountains for global comparative mountain science, *Sci Data*, 9, 149, <https://doi.org/10.1038/s41597-022-01256-y>, 2022.
- Sujud, L. and Jaafar, H.: A global dynamic runoff application and dataset based on the assimilation of GPM, SMAP, and GCN250 curve number datasets. *Sci Data*, 9(1), p.706, <https://doi.org/10.1038/s41597-022-01834-0>, 2022.
- Tadono, T., Ishida, H., Oda, F., Naito, S., Minakawa, K., and Iwamoto, H.: Precise Global DEM Generation by ALOS PRISM, *ISPRS Annals of the Photogrammetry, Remote Sensing and Spatial Information Sciences*, II–4, 71–76, <https://doi.org/10.5194/isprsannals-ii-4-71-2014>, 2014.
- Thornton, J.M., Palazzi, E., Pepin, N.C., Cristofanelli, P., Essery, R., Kotlarski, S., Giuliani, G., Guigoz, Y., Kulonen, A., Pritchard, D. and Li, X.: Toward a definition of essential mountain climate variables. *One Earth*, 4(6), pp.805–827, <https://doi.org/10.1016/j.oneear.2021.05.005>, 2021.
- Thornton, J.M., Snethlage, M.A., Sayre, R., Urbach, D.R., Viviroli, D., Ehrlich, D., Muccione, V., Wester, P., Insarov, G. and Adler, C.: Human populations in the world's mountains: Spatio-temporal patterns and potential controls. *PLoS One*, 17(7), p.e0271466, <https://doi.org/10.1371/journal.pone.0271466>, 2022.
- Viviroli, D., Kumm, M., Meybeck, M., Kallio, M., and Wada, Y.: Increasing dependence of lowland populations on mountain water resources. *Nature Sustainability*, 3(11), 917–928, <https://doi.org/10.1038/s41893-020-0559-9>, 2020.
- Xiong, L., Li, S., Tang, G., and Strobl, J.: Geomorphometry and terrain analysis: Data, methods, platforms and applications, *Earth-Science Reviews*, 104191, <https://doi.org/10.1016/j.earscirev.2022.104191>, 2022.
- Xiong, L., Li, S., Hu, G., Wang, K., Chen, M., Zhu, A. and Tang, G.: Past rainfall-driven erosion on the Chinese loess plateau inferred from archaeological evidence from Wucheng City, Shanxi. *Communications Earth & Environment*, 4(1), p.4, <https://doi.org/10.1038/s43247-022-00663-8>, 2023.
- Yang, X., Li, S., Ma, J., Chen, Y., Zhou, X., Zhou, C., Meadows, M., Li, F., Xiong, L., Tang, G.: Global Relief Clasess (GRC) Dataset, Zenodo [data set], <https://doi.org/10.5281/zenodo.15641257>, 2024.
- Yu, L., Wang, J., and Gong, P.: Improving 30 m global land-cover map FROM-GLC with time series MODIS and auxiliary data sets: a segmentation-based approach, *International Journal of Remote Sensing*, 34, 5851–5867, <https://doi.org/10.1080/01431161.2013.798055>, 2013.
- Zhou, C. H., Cheng, W. M., Qian, J. K., Li, B. Y., and Zhang, B. P.: Research on the classification system of digital land geomorphology of 1: 1000000 in China, *Journal of Geo-Information Science*, 11, 707–724, <https://doi.org/10.3724/SP.J.1047.2009.00707>, 2009.
- Zhou, Z., and Chen, Y.: How urban land expansion alters terrain in mountainous and hilly areas: An empirical study in China. *Geography and Sustainability*, 100304, <https://doi.org/10.1016/j.geosus.2025.100304>, 2025.